

 Open access • Journal Article • DOI:10.1007/S11356-021-13265-2

Modelling of impact of presence/absence of suspended particulate organic matter from river and sea and effluent wastewater on fluorescence signal in the coastal area of Gapeau River — Source link

Ibrahim El-Nahhal, Roland Redon, Michel Raynaud, Yasser El-Nahhal ...+1 more authors

Institutions: Aix-Marseille University, Islamic University

Published on: 11 Mar 2021 - Environmental Science and Pollution Research (Springer Berlin Heidelberg)

Related papers:

- [Effects of sampling methods on the quantity and quality of dissolved organic matter in sediment pore waters as revealed by absorption and fluorescence spectroscopy](#)
- [Fluorescence Analysis for Measurement of Dissolved Organic Matter in Environmental Water](#)
- [Fluorescence spectroscopy and parallel factor analysis as a dissolved organic monitoring tool to assess treatment performance in drinking water trains.](#)
- [Dissolved organic matter in hand-dug well water as groundwater quality indicator: assessment using laser-induced fluorescence spectroscopy and multivariate statistical techniques](#)
- [Fluorescence-based multi-parameter approach to characterize dynamics of organic carbon, faecal bacteria and particles at alpine karst springs.](#)

Share this paper:    

View more about this paper here: <https://typeset.io/papers/modelling-of-impact-of-presence-absence-of-suspended-22pmb00trw>



HAL
open science

Modelling of impact of presence/absence of suspended particulate organic matter from river and sea and effluent wastewater on fluorescence signal in the coastal area of Gapeau River

Ibrahim El-Nahhal, Roland Redon, Michel Raynaud, Yasser El-Nahhal,
Stéphane Mounier

► To cite this version:

Ibrahim El-Nahhal, Roland Redon, Michel Raynaud, Yasser El-Nahhal, Stéphane Mounier. Modelling of impact of presence/absence of suspended particulate organic matter from river and sea and effluent wastewater on fluorescence signal in the coastal area of Gapeau River. *Environmental Science and Pollution Research*, Springer Verlag, In press, 10.1007/s11356-021-13265-2 . hal-03171038

HAL Id: hal-03171038

<https://hal.archives-ouvertes.fr/hal-03171038>

Submitted on 16 Mar 2021

HAL is a multi-disciplinary open access archive for the deposit and dissemination of scientific research documents, whether they are published or not. The documents may come from teaching and research institutions in France or abroad, or from public or private research centers.

L'archive ouverte pluridisciplinaire **HAL**, est destinée au dépôt et à la diffusion de documents scientifiques de niveau recherche, publiés ou non, émanant des établissements d'enseignement et de recherche français ou étrangers, des laboratoires publics ou privés.

1 Manuscript prepared for possible publication in ESPR 04-12-2020

2

3

4

5

6

7 **Modelling of impact of presence/absence of suspended particulate organic matter from river and sea and efflu-**
8 **ent wastewater on fluorescence signal in the coastal area of Gapeau River**

9

10

11

12

13

14

15 Ibrahim EL-Nahhal^a, Roland Redon^a, Michel Raynaud^a, Yasser EL-Nahhal^b, Stéphane Mounier^a

16 ^a Université de Toulon, Aix Marseille Univ, CNRS, IRD, MIO - CS 60584, 83041 TOULON CEDEX 9, France

17 ^b Department of Environmental and Earth Sciences, Faculty of Science, The Islamic University-Gaza, P.O Box 108,
18 00970 Palestinian Territories.

19 *Corresponding author: elnahhal.i@gmail.com (Ibrahim Y. Z. EL-Nahhal)

20 *Corresponding author ORCID: <https://orcid.org/0000-0002-3321-7359>

21 **Abstract:**

22 Organic matter has an important role in biogeochemistry in aquatic environments. This study investigated impact of
23 suspended particulate organic matter (SPOM) on fluorescence signal of mixtures of three water types (River water
24 RW, Sea water SW, effluent wastewater WW) using three-dimensional excitation emission fluorescence spectroscopy
25 (3D-EEMs) and Parallel factor analysis PARAFAC and multilinear regression. Four irradiation experiments (Exp.1,
26 Exp.2, Exp.3 and Exp.4) were conducted during different times of year (two in autumn, one in winter and one in
27 spring season). Samples were exposed to natural sunlight on laboratory rooftop in University of Toulon, France, with
28 another set of samples were kept in dark as control samples. Three components (C1,C2, C3) model was validated by
29 split-half and Concordia from the whole EEM dataset of all irradiation experiments. No protein-like fluorophores or
30 PARAFAC components was found. The study revealed the effect of SPOM presence/absence on fluorescence signal
31 of DOM and on resulting parameters of multilinear regression MLR model and kinetic constant of these MLR param-
32 eters. Kinetic constant (k) for all MLR coefficients was in order of greatness as Exp.1 (SPOM of WW only in mixtures
33) > Exp.3 (SPOM of SW only in mixtures) > Exp.2 (SPOM of RW only in mixtures)> Exp.4 (All SPOM of RW, SW,
34 WW in mixtures) indicating that SPOM of WW is the most resistant to photodegradation. For dark control samples,
35 only relative standard deviation RSD could be calculated from dataset. RSD values for C3 were the highest indicating
36 its chaotic variations and the lowest RSD values were found for both C1 and C2 for all experiments. Statistical differ-
37 ences has been found between control and irradiated experiments. These models developed in this study can be used
38 to predict fluorescence signal of anthropogenic effluent DOM during its transport in river systems to coastal zone.

39 **Keywords:**

40 Suspended Particulate Organic matter SPOM, Fluorescence Spectroscopy, parallel factor analysis PARAFAC model-
41 ing, Solar Irradiation, mixing experiments.

42 **Introduction**

43 Organic matter in natural waters can be operationally classified and divided into dissolved organic matter (DOM) or
44 suspended particulate organic matter (SPOM) depending on the filtration and filter size (Osburn et al., 2012; Gagné
45 and Tremblay 2009). DOM pool consists of a wide range of organic molecules originating from decaying dead stuff
46 (plants and animals). Such organic molecules could be humic substances (i.e. humic and fulvic acid) or non-humic
47 substances such as proteins, and carbohydrates with varying molecular size and functional groups (Her et al. 2003).
48 Whereas, SPOM pool may consist of living microorganisms (e.g. bacteria and viruses), organic/inorganic particles
49 organic polymers among others (Chin et al. 1998; Leppard et al. 2011). SPOM in water plays an important role in
50 characterizing the fate of (DOM) in ecosystems. SPOM and DOM are an important constituent in aquatic environments
51 and plays a significant role in the transport, stability and bioavailability of several organic/inorganic pollutants that
52 results from anthropogenic activity (e.g. heavy metals, pesticides and polycyclic aromatic hydrocarbons) (Akkanen et
53 al. 2004; Hirose 2007; Baker et al. 2008; Ishii and Boyer 2012). However, DOM in aquatic ecosystems is considered
54 to be the most important and significant fraction of organic matter due to its involvement in so many environmental
55 processes (Søndergaard and Thomas, 2004)

56 In addition, both of them have a role in global biogeochemical cycling of carbon and nutrients. It is critical for the
57 better understanding of carbon cycle to differentiate sources of DOM in aquatic environment and the factors which
58 play important roles in its sources and sinks like biodegradation and photodegradation (McCallister et al. 2006a,b;
59 Dalzell et al. 2009). More research attention has been given to study the role in environmental photochemistry of
60 DOM than that of SPOM (Mopper et al. 2014). Solar irradiation of (SPOM) may result in production of dissolved
61 nutrients and/or DOM in considerable amounts which may enrich the aquatic system. For instance, previous studies
62 (Liu and Shank 2015; Mayer et al. 2006; Riggsbee et al. 2008; Southwell et al. 2010; Estapa and Mayer 2010; Pisani
63 et al. 2011) investigated the influence of sunlight on POM and found that it undergo similar photochemical reactions
64 as DOM due to absorbance of UV-VIS light which are the same wavelengths that DOM can absorb. Moreover, He et
65 al. (2016) evaluated the effect of SPOM in attenuating the fraction of dissolved organic carbon and revealed that SPOM
66 can reduce the concentration of dissolved organic carbon in water systems through adsorption process. Moreover,
67 influence of SPOM in fluorometry of DOM were investigated by several authors (e.g. Laane and Kramer 1990; De
68 Souza Sierra and Donard 1991; Baker and Spencer 2004; Boyd and Osburn 2004; Callahan et al. 2004; Kowalczuk et
69 al. 2003, 2005; Murphy et al. 2008). Evolution of fluorophores of DOM (i.e. FDOM) is being followed using spectro-
70 fluorometry which is a qualitative and semi-quantitative technique. Spectrofluorometry technique of three-dimensional
71 excitation–emission matrix (EEM) spectroscopy has several advantages for the detection of fluorophores of DOM in

72 aquatic environment because it is fast and non-destructive with no need for sample pre-treatment and is highly sensitive
73 for detection of even-low concentrations of samples which is the case in several aquatic environments. In addition to
74 the fact that type and origin of samples (riverine , marine, wetlands) can be figured out and types and relative concen-
75 trations of fluorophores constituting DOM can also be known using three-dimensional excitation–emission matrix
76 (EEM) spectroscopy.

77 Previous studies (He et al. 2016) investigated the influence of SPOM in light scattering, adsorption of DOM, attenua-
78 tion of dissolved organic carbon and other matters, however the impact of presence/absence of SPOM on fluorescence
79 signal of naturally occurring mixtures is not fully understood. Accordingly, this study was designed to bridge the gap
80 of knowledge in the field of SPOM effect on fluorescence signal of naturally occurring mixtures of river water and
81 effluent wastewater and sea water. Therefore, the research question of this study is that will the presence/absence of
82 particulate matter from one of three water types (river water, seawater, effluent wastewater) affect the modelling and
83 kinetics of degradation of fluorescence signal of different mixtures of these water types after solar irradiation . So far,
84 the objectives of this study are to investigate the effect of presence/absence of SPOM on fluorescence signal of natu-
85 rally occurring mixtures through mixing experiments and to examine the impact of solar photodegradation on mixtures
86 of different types of water (i.e. river water RW, Sea water SW and wastewater effluent WW) by using the technique
87 of three-dimensional fluorescence spectroscopy and parallel factor analysis PARAFAC by developing a multilinear
88 regression model for tracking the effect of SPOM on fluorescence signal of the above mentioned mixtures to simulate
89 naturally occurring mixing in coastal zone which could be used in further work to develop online or real-time remote-
90 sensing monitoring software.

91 **Material and methods**

92 **Study area and Sample Collection**

93 Gapeau river, a small coastal river, is situated in Var department in Provence-Alpes-Côte d'Azur region located in
94 Southeastern France and is the second largest river in Var department. It discharges its runoff in Mediterranean Sea at
95 Hyeres City. It is submitted to various anthropogenic inputs especially thirteen wastewater treatment plants in its water
96 catchment. In this study, the focus was on anthropogenic organic matter from La Crau wastewater treatment plant
97 WWTP which served 50,086 inhabitants. This WWTP uses secondary and tertiary technologies for wastewater
98 treatment such as activated sludge technology, sand filter, prolonged aeration and anaerobic sludge digestion.
99 Sampling was done using plastic bottles of one liter each to sample 1 liter of River water , wastewater treatment plant
100 effluent and Sea water. Exact GPS locations of these sampling sites are the same according to recent procedures (EL-
101 Nahhal et al. 2020). Eight sampling cruises were conducted for solar irradiation experiments, sampling dates

102 corresponding to each irradiation experiment are shown in Table 2.

103 **Collected Samples Filtration**

104 Having three types of water (River water RW, Sea water SW and wastewater effluent WW) and making permutations
105 of filtering of two types of water and leaving the last one non-filtered, we end up with experiments described in Table
106 2. Filtration process (Removal of SPOM) was conducted using a filtration kit and MilliPore filters (Type GNWP 0.20
107 μm , 47 mm diameter) to filter (one liter) 1L of RW and 1L SW and leaving 1L of WW not filtered (Exp. 1 in table 2)
108 to investigate the impact of SPOM from this non-filtered WW on mixtures (prepared according to the next section in
109 Materials and methods). Experiment Exp.2 indicates that 1L of RW was not filtered and the other two 1L of SW and
110 1L of WW were filtered to study the impact of these SPOM coming from river water RW on mixtures (the following
111 section). The same goes for remaining experiments in table 2.

112 **Preparing water mixtures**

113 Vials of quartz were used because quartz allows absorption of UV-VIS energy. Different mixing percentages taken
114 from the collected 1L RW, 1L SW and 1L WW (filtered or not filtered as explained in the previous section) were taken
115 by pipette and inserted in quartz vial according to table 1 (or Fig.1). These mixing percentages are speculated to
116 represent actual mixing in nature. After having the required mixing percentages, all quartz vials were hand-shaken to
117 have representative mixtures. Another fifteen control samples had the same mixing percentages and prepared in dark
118 vials. Each intersection point and summits in the ternary diagram in Fig.1 represents a corresponding quartz vial that
119 contains the indicated percentages in the ternary diagram of mixtures. Exact volume of RW, SW and WW in each
120 quartz vial is indicated in Table 1. Total volume of each quartz vial is 50 mL.

121 **Measurements of DOC and POC and UV-Vis spectra**

122 Shimadzu TOC-5000A Total Organic Carbon Analyzer (catalytic combustion) with module ASI-5000A has been used
123 to measure dissolved organic carbon (DOC) at high temperature (720 °C) and with module SSM-5000A to measure
124 particulate organic carbon (POC). Acidification was performed to $\text{pH} < 2$ using 2 N HCl on samples of 1L RW, 1L
125 SW and 1L WW in each irradiation experiment and CO_2 was removed by purging samples with oxygen. UV-visible
126 absorption spectra (between 250–800 nm) were measured using a PerkinElmer Lambda 10500 UV/VIS spectropho-
127 tometer with a 1 cm quartz cuvette with the blank as MilliQ water for the series of dilutions (100%, 50%, 25%, 12,5%)
128 of 1L RW, 1L WW, 1LSW to check for inner filter effect according to Tucker et al. (1992).

129 **Irradiation experiments**

130 Four irradiation experiments were conducted at different time of year (Table 2). The first two experiment were
131 conducted in autumn and in winter season, and the last one was conducted in spring and the exact dates are described

132 in (Table 2). Fifteen mixtures in quartz vials (according to previous section) were prepared and transferred on rooftop
133 of our laboratory MIO at Campus La Garde, Universite de Toulon in plank at sufficient distances from each other to
134 have the same irradiation conditions as shown in Fig.2. The used apparatus for these experiments is shown in Fig.2.
135 Another fifteen control samples were prepared and incubated in dark box in vicinity of irradiated samples.

136 **Measurements of light intensity.**

137 Météo-France (www.meteofrance.com) provided solar irradiance (light intensity) measured in milliVolts mV for each
138 day of irradiation as mentioned in table 2 and the cumulative light intensity was calculated and graphed for each
139 irradiation experiment.

140 **Excitation Emission Matrix EEM fluorescence spectroscopy**

141 Spectrofluorometric measurements were completed using a 1-cm quartz cuvette with a Hitachi F-4500 spectrofluoro-
142 rometer with PMT voltage of 700 V, at 25 °C and sampling using a pipette a 3 mL from each irradiated quartz vial. A
143 correction for the change in volume was done by replacing the taken 3mL aliquots by another 3 mL of deionized water
144 therefore steady state concentration was kept till the end of each irradiation experiment. Sodium azide (100 µL of 1M
145 NaN₃) was added for each sampled 3mL to inhibit biodegradation during EEM fluorescence measurements. Addition
146 of sodium azide NaN₃ has no effect on fluorescence intensity in EEMs as revealed by Patel-Sorrentino et al. (2002).
147 Excitation wavelengths (Ex) spectra were measured from 200 to 400 nm at 5 nm-increment, and emission wavelengths
148 (Em) spectra from 220 to 420 nm at 5 nm-intervals with scan speed set at 2,400 nm.min⁻¹. Slit width of 5 nm was set
149 for both excitation and emission wavelengths. EEM datasets of solar irradiation experiments were processed using
150 Matlab 2013a (Math Works Inc., USA). All recorded EEMs were blank-corrected through the subtraction of EEMs of
151 Sealed ultrapure Perkin Elmer deionized water cell. Integrated Raman signal of Sealed ultrapure Perkin Elmer deion-
152 ized water cell was used to normalize values of each excitation-emission matrix and it was calculated by integrating
153 the area under the curve from 370 to 420 nm (Lawaetz and Stedmon 2009). All fluorescence intensity were in Raman
154 units (RU) . Only EEMs before irradiation of Samples No. 1,2 and 3 in table 1 are presented in the results and discus-
155 sion section whereas the remaining EEMs are not shown since the total number of EEMS for all four irradiation
156 experiments is 648 EEMs.

157 **Parallel factor analysis (PARAFAC) of EEM data**

158 PARAFAC is a powerful multiway technique used to decompose and fully make use of the EEM dataset. The principle
159 of PARAFAC is that it decomposes any given EEM dataset into its underlying EEM spectra constituents (Murphy et
160 al. 2013) which are a set of trilinear terms and a residual array using an alternating least squares algorithm to minimize
161 sum of squared residuals in a trilinear model. Resulting PARAFAC components represents fluorophores having similar

162 fluorescing properties which constitute the EEM dataset. PARAFAC modeling was performed on the whole EEM
 163 datasets of all irradiation experiments (Table 2) using MATLAB software (MathWorks R2015b, USA) and NWAY
 164 toolbox and DOMFluor toolbox (<http://www.models.life.ku.dk>) (Micó et al. 2019; Stedmon and Bro 2008) for a total
 165 of 648 EEMs. Numerical filter was taken as 25 nm to eliminate Raman and Rayleigh scattering according to Zepp
 166 method (Zepp et al. 2004). Based on CONCORDIA score, split- half analysis and visual inspection of spectral shapes
 167 of each PARAFAC component, the accepted number of PARAFAC components was determined (Bro 1998). Split-
 168 half analysis were performed for validation of PARAFAC model results (Stedmon et al. 2003; Murphy et al. 2013).
 169 Scores of each PARAFAC component represent relative concentration of each PARAFAC component in EEM dataset.
 170 Quantitative and qualitative variations of the composition of organic matter can be extracted from PARAFAC
 171 modelling of EEM datasets. Normalization of contributions of PARAFAC components was performed by dividing
 172 each contribution with its corresponding daily maximum contribution.

173 **Multilinear regression between scores of PARAFAC components and f_{RW} and f_{SW}**

174 Based on the explanation recently described (EL-Nahhal et al. 2020), the final multilinear regression equation as a
 175 function of f_{RW} and f_{SW} is:

$$C^*_i = A^{WW}_{i,0} + A^{WW}_{i,1} \cdot f_{SW} + A^{WW}_{i,2} \cdot f_{RW} \quad (\text{Eq.1})$$

176 Where f_{RW} and f_{SW} are percentages in mixture in a given quartz vial of RW and SW as described in Fig.1;

177 $A^{WW}_{i,0}$, $A^{WW}_{i,1}$ and $A^{WW}_{i,2}$ represent multilinear regression coefficients related to mixing equation when f_{RW} is
 178 expressed in terms of percentages (f_{RW} and f_{SW}). i is the number of a given PARAFAC component (e.g. C1, C2, C3).

179 More details and explanations are thoroughly given elsewhere (EL-Nahhal et al. 2020).

180 **Kinetics of Multilinear regression parameters $A^{WW}_{i,0}$, $A^{WW}_{i,1}$ and $A^{WW}_{i,2}$**

181 $A^{WW}_{i,0}$, $A^{WW}_{i,1}$ and $A^{WW}_{i,2}$ values change for each day of irradiation in a given experiment. Changes in their values
 182 were modeled to rate order kinetic equation in order to get a model for the evolution of fluorescence signal as a
 183 function of irradiation energy expressed in volts V; with their kinetic formulas expressed as $A^{WW}_{i,0}(V)$, $A^{WW}_{i,1}(V)$
 184 and $A^{WW}_{i,2}(V)$.

185 Accordingly, multilinear regression model in eq. 1 can be expressed kinetically as follow:

$$C^*_i(V) = A^{WW}_{i,0}(V) + A^{WW}_{i,1}(V) \cdot f_{SW} + A^{WW}_{i,2}(V) \cdot f_{RW} \quad 2)$$

186 **Statistical Analysis**

187 Multi-regression analysis was used to investigate the strength of linear relationships between concentration scores of
188 fluorescent components obtained from PARAFAC analysis and water mixing composition. Regression and correlation
189 analyses and relative standard deviation for multilinear regression parameters in control non-irradiated samples were
190 performed using Microsoft Excel 2016. Significances of correlations in the statistics were evaluated.

191 **Results and Discussions**

192 Measured light intensity in mV for Exp.1, Exp.2, Exp.3 and Exp.4 are presented in Fig.3. It can be noticed from Fig.3
193 that light intensity in Exp.1 which was conducted in autumn and the third one Exp.3 which was conducted in winter
194 season have the lowest light intensity compared to Exp.2 (conducted in autumn) and Exp.4 (conducted in spring). The
195 high light intensity in autumn Exp.2 in December 2015 compared to autumn Exp.1 in November 2015 is due to un-
196 predictable weather in PACA (Provence Alpes Cote d'Azur) region in southeastern France. This explains the rapid
197 photodegradation in Exp.2 and Exp.4.

198 **UV-VIS Absorption spectra of 1L RW, 1L WW, 1L SW**

199 UV-VIS absorption spectra of sampled 1-liter river water RW, 1-liter effluent wastewater WW and 1-liter seawater
200 and the dilution series 100%, 50%, 25% and 12,5% for each water type are shown in Fig. 4. It can be seen from Fig 4
201 that UV-VIS absorption spectrum of all water types RW, WW and SW decrease linearly with dilution series (100%,
202 50%, 25% and 12,5%) showing no primary or secondary inner filter effect in these waters (RW,WW & SW) as
203 previously described (Tucker et al. 1992; Ohno 2002). In addition, sand filter; a tertiary wastewater treatment
204 technology; is used in the WWTP of La Crau city in this study removes inner filter effect caused by SPOM and this is
205 in accordance with Sgroi et al. (2020) who found no inner filter effect for effluent tertiary wastewater after sand
206 filtration.

207 **Excitation Emission Matrix of Example Samples 1,2 and 3 before irradiation and after irradiation**

208 Collected water samples (RW, SW and WW) have different origin to match the naturally occurring mixtures. Filtration
209 of samples was done to match naturally occurring precipitation in ecosystems. For instance, at rough sea water
210 movement, SPOM are at most whereas, at soft sea, SPOM tend to precipitate resulting in as clean solution as filtrated
211 samples. Moreover, the use of different irradiation periods is to understand the effects of different light intensities on
212 degradation processes and fluorescence signal of DOM. Three-dimensional fluorescence spectra (EEMs) of the first
213 three samples in table 1 are presented for every irradiation experiment in Figures (5, 6, 7 and 8) as example EEMs of
214 the effect of solar irradiation (the remaining EEMs for each sample in table 1 are not shown).

215 **First experiment Exp.1 (in autumn) .**

216 First irradiation experiment (Exp. 1) was conducted in the autumn season starting irradiation from November 10 to

217 November 20 2015 (Table 2). EEMs of Samples no 1, 2 and 3 in table 1 (before irradiation and after irradiation and
218 the difference between before and after irradiation) are presented in Fig.5 for Exp.1 in which SPOM from effluent
219 WW is present whereas SPOM from RW and SW were absent. Concentrations of POC of WW was 3 ± 0.23 mg/l
220 whereas DOC concentration of RW and SW were 2.1 ± 0.18 mg/l and 2.4 ± 0.19 mg/l. It can be seen in Fig. 5 that
221 unfiltered and unmixed effluent WW (sample no. 3) contains the highest fluorescence intensities before irradiation
222 and after irradiation compared to samples no. 1 and 2. All fluorescence peaks got photodegraded as shown by the
223 diminution of fluorescence intensity of them as clearly can be seen in color bar values.

224 **Second experiment Exp. 2 (in autumn)**

225 Second irradiation experiment (Exp. 2) was also conducted in autumn season starting irradiation from December 20
226 until December 17 2015 (Table 2). EEMs of Samples no 1, 2 and 3 in table (before irradiation and after irradiation and
227 the difference between before and after irradiation) are presented in Fig.6 for Exp. 2 in which particulate organic matter
228 from river water is present whereas seawater and effluent wastewater were filtered. The concentration of POC of RW
229 was 0.5 ± 0.14 mg/l whereas DOC concentration of SW and WW were 2 ± 0.3 mg/l and 3.5 ± 0.2 mg/l. It can be seen in
230 Fig.6 that peak C representing humic-like fluorophores and peak M representing marine humic-like fluorophores
231 (Coble 1996) has medium intensity in sample no. 1 (unmixed RW i.e. 100% RW) and higher intensity peak C in the
232 sample no. 2 (unmixed SW i.e. 100% SW) and the highest intensity found in sample no.3 (unmixed WW). In addition,
233 peaks B and T which represent protein-like fluorophores (tyrosine-like and tryptophan-like) are also higher in
234 fluorescence intensity compared to samples no. 1 and 2 before irradiation. After irradiation, fluorescence intensity of
235 peak B (tyrosine-like fluorophores) and peak T (Tryptophan-like fluorophores) degraded as shown with their lowest
236 fluorescence intensities shown as the values in the color bar. Furthermore, the light intensity in the second experiment
237 in autumn is less than the light intensity in experiment Exp.1. This suggest slower photochemical degradation.

238 **Third experiment Exp. 3 (in winter season)**

239 Third irradiation experiment (Exp. 3) was conducted in the winter season starting irradiation from February 15 until
240 March 4 2016 (Table 2). EEMs of Samples no 1, 2 and 3 in table (before irradiation and after irradiation and the
241 difference between before and after irradiation) are presented in Fig.7 for Exp. 3 in which particulate organic matter
242 from sea water is present whereas river water and effluent wastewater were filtered. The concentration of POC of SW
243 was 0.6 ± 0.07 mg/l whereas DOC concentration of RW and WW were 2 ± 0.18 mg/l and 3.7 ± 0.14 mg/l. It can be seen
244 in Fig.7 that sample no 2 (unmixed and unfiltered SW) has the lowest fluorescence intensity for most peaks (C, A, M,
245 B, and T) before irradiation and sustained more or less the same fluorescence intensity after irradiation. There was no
246 inner-filter effect in this sample as checked by UV-VIS absorption spectra of SW as explained above. For filtered WW
247 (sample no. 3), it is characterized by the highest fluorescence intensities (before irradiation and after irradiation)

248 compared to samples no 1 and 2. Moreover, peaks C and M degraded the most which is in agreement with Zhu et al.
249 (2017b) who found that CDOM from terrestrial origins was more susceptible to photochemical degradation compared
250 to CDOM from biological sources.

251 **Fourth experiment Exp.4 (in spring season)**

252 Last irradiation experiment (Exp. 4) was conducted in spring season starting irradiation from May 05 until May 27
253 2016 (Table 2). EEMs of Samples no 1, 2 and 3 in table (before irradiation and after irradiation and the difference
254 between before and after irradiation) are presented in Fig.8 for Exp.4 in which particulate organic matter from RW,
255 SW and WW are present at the same time in all the samples of Table 1. Concentrations of POC of RW, SW and WW
256 were $0.6\pm 0.1\text{mg/l}$, $0.7\pm 0.2\text{mg/l}$ and $2.75\pm 0.45\text{mg/l}$. It can be seen in Fig.8 that the highest fluorescence intensity is
257 found in Sample No.3 (100% WW) which is characterized by high peak C and M intensities which are degraded after
258 irradiation. This finding is in accord with previous report (Seong-Nam and Gary 2008). The too low fluorescence
259 intensities of protein-like peaks in all the EEMS shown in figures (Fig. 5, 6, 7 and Fig.8) are in accordance with the
260 results of PARAFAC model shown in Fig.9 where there was no protein-like PARAFAC component was found.

261 **Parallel factor analysis (PARAFAC) of EEM data**

262 EEMs of fifteen samples (Table 1) for each irradiation day and for all the irradiation experiments (Exp.1, Exp.2, Exp.3
263 and Exp.4) have been decomposed using PARAFAC for a total of 648 EEMs. PARAFAC decomposition of 648 EEM
264 dataset of all irradiation experiments (Table 2) gives three independent components which are validated by
265 CORCONDIA 74.9 % and split-half method. Fluorescence landscape of PARAFAC components (C1, C2 and C3)
266 with corresponding excitation and the emission loadings are shown in Fig.9. It can be noticed that the nature of
267 PARAFAC components seem to be present with varying contributions in every sample in the whole EEMs dataset of
268 all Irradiation experiments. Excitation emission loadings of each component (C1, C2 and C3) were compared with
269 Openfluor.org database and previously reported PARAFAC components in literature and their corresponding
270 equivalents are shown in Table 3. C1 presented excitation maximum at 340 nm and an emission maximum at 430 nm.
271 Previous studies have associated this component to UV-A humic-like fluorophores and Peak C (Coble 1996) and peak
272 “ α ” (Parlanti et al. 2000). It represents terrestrial humic-like and it can be suggested that it is used as wastewater/nutrient
273 enrichment tracer (Murphy et al. 2011). C2 showed excitation maximum at 375 nm and an emission maximum at 465
274 nm. This component represents more humified fluorophores and resembles C2 found in the study of (Abaker et al.
275 2018) and it is of fluvic-like fluorophores Peak A (Coble 1996). C3 excitation/emission peak was located at
276 wavelengths of 295/405nm. This may be attributed to anthropogenic humic materials, agricultural and microbial
277 component. This component C3 was defined in literature as marine humic-like peak M (Coble, 1996) and has
278 resemblance to Q3 which is a microbially oxidized component (Cory and McKnight 2005). This suggestion is in

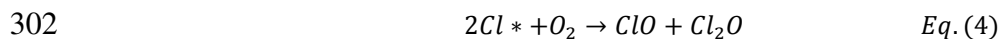
279 accordance with previous reports (Murphy et al. 2008; Stedmon and Markager 2005). Furthermore, no protein-like
 280 component was detected by PARAFAC which is validated by split-half method. The above-described PARAFAC
 281 fluorescent components were used to reconstruct the original whole EEMs dataset and for multilinear regression
 282 between each component (i.e. C1, C2 and C3) and sample composition (f_{SW} and f_{RW}).

283 **Photochemical variation in fluorescent PARAFAC components**

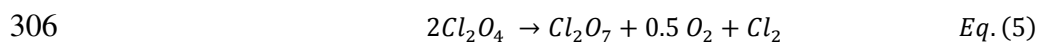
284 Variation of C1, C2 and C3 in irradiation experiment Exp.4 before conducting multilinear regression indicates how
 285 the parameters of multilinear regression varies with irradiation process. Changes of maximum fluorescence intensity
 286 F_{max} of each PARAFAC components with irradiation time are shown in Fig.10. Fig.10 shows variations of F_{max} for C1,
 287 C2 and C3 which decrease with irradiation process which is very clear for irradiated samples (shown in black).
 288 Whereas, for control samples (dark) (shown in dotted gray), F_{max} doesn't have a clear trend which explains the results
 289 presented in Fig.11. Similar trend has been found for the remaining irradiation experiments (Exp.1, Exp.2, Exp.3 and
 290 Exp.4) (data not shown). These findings suggest that photodegradation impact humic and fluvic-like fluorophores in
 291 water column in river and sea water. Additionally, SPOM may adsorb soluble organic matter from water resulting in
 292 a photoprotection to the DOM. This process may result in reducing photochemical degradation in which the
 293 fluorescence signal is not dramatically affected. In this regard, we suggest the following protection mode from
 294 suspended particulate organic matter. As many wastewater treatment plants use chlorine as a disinfectant material
 295 after secondary treatment and seawater in France is partly chlorinated (Péron and Courtot-Coupez 1980). Part of the
 296 added chlorine may undergo the following reaction either in treatment plants or receiving water bodies. Under sunlight,
 297 chlorine in effluent wastewater samples undergo the following reactions according to equations 3 and 4.
 298 Photodegradation of Cl_2 under sunlight produces free radicals of as shown in Eq. (3).



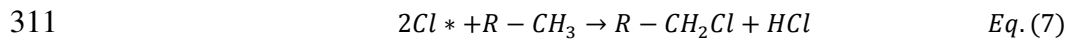
300 Free radicals produced in Eq. 3 react with oxygen to produce chlorine oxides may be classified in monochlor- and
 301 dichloroxi- derivatives as previously reported (Lopez et al., 1998) (Eq. 4)



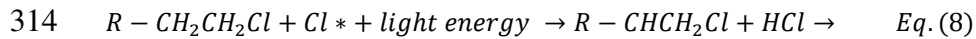
303 All these compounds are thermally unstable and may decompose readily in atmosphere. Nevertheless, these reactions
 304 are contentious and may lead to formation of Cl_2O_4 which may undergo a reformation reaction to reproduce Cl-Cl
 305 undergo continues reaction as shown in Eq. 5-6.



308 These proposed reactions are in accordance with Lopez et al., 1998 who indicated formation of these photochemical
309 reaction under exposure to light at wavelength of 366 nm. So far, free radicals produced in Eq. 3 react with dissolved
310 organic matter (Glucose, fatty acid and or protein) producing organochlorine compound according to Eq. (7)



312 These chlorinated hydrocarbons (R-CH₂Cl) are persistent in ecosystem and are able to absorb solar energy and release
313 it again into environment to go to its stable stage according to Eq. 8.



315 The produced compound R-CHCH₂Cl is fluorescent matter due to double bond formation. Where R can be an aliphatic
316 or aromatic moiety (Margulies et al. 1994). Presence of particulate matter in the system can reduce the rate of above-
317 mentioned reactions (3-8) but cannot stop them. The proposed reactions agree with previous reports (Morris 1978; El-
318 Nahhal et al. 1999 ; Nir et al. 2000 ; Muellner et al. 2007) and recent reports (Yuan et al. 2020)

319 **Initial values of (A^{ww*0} , A^{ww*1} , A^{ww*2}) before irradiation**

320 Values of multilinear regression coefficients for PARAFAC components (C1, C2 and C3) are given in table 4 for time
321 zero, i.e. before the start of irradiation experiments, for all irradiation/mixing experiments. Multilinear regression
322 between (C1,C2 and C3) and (f_{sw} , f_{rw}) shows excellent fitting since the power of correlation is high as indicated from
323 values of r^2 for each irradiation experiment as shown in table 4. It can be seen that values of intercept ($A^{ww}_{1,0}$, $A^{ww}_{2,0}$,
324 $A^{ww}_{3,0}$) are of two order of magnitude higher than the absolute value of both coefficients of f_{sw} ($A^{ww}_{1,1}$, $A^{ww}_{2,1}$,
325 $A^{ww}_{3,1}$) and f_{rw} ($A^{ww}_{1,2}$, $A^{ww}_{2,2}$, $A^{ww}_{3,2}$) for all PARAFAC components. The intercept ($A^{ww}_{1,0}$, $A^{ww}_{2,0}$, $A^{ww}_{3,0}$)
326 contains implicitly the impact of f_{ww} on resulting fluorescence contribution of (C1, C2 and C3) as explained thoroughly
327 in the methodology section of this manuscript . This indicates that increasing f_{sw} or f_{rw} result in decreasing the resulting
328 fluorescence contribution of (C1, C2 and C3). Additionally, it can be suggested that presence of particulate matter
329 slows the intensity of photochemical degradation, this is quite obvious with the slight changes in samples that contains
330 large fraction of suspended particulate matter compared with filtrated samples. Furthermore, suspended organic matter
331 may adsorb dissolved organic matter on its surfaces and provide photoprotection from degradation. This phenomenon
332 is in accordance with previous reports (EL-Nahhal et al. 2001; Nir et al. 2000; Margulies 1996) that revealed the ability
333 of organoclay complexes to provide photoprotection to photodegradable pesticides. Moreover, filtration of samples
334 may increase the contribution of fluorescence of mixing process is predominated by wastewater treatment plant for
335 PARAFAC components and filtration has a measurable effect on multilinear regression parameters. When SPOM of
336 only one water source is present, there is a decrease of values of the intercept parameter which suggest that there is an
337 effect on fluorophores of filtered particles. When SPOM from RW is present (i.e. Exp.2), values of intercept are greater

338 than that when SPOM from SW (i.e. Exp.3) is present suggesting that removal of fluorophores of river water plays a
339 role on values of intercept. In general, there is an influence of presence/absence of SPOM on the initial contribution
340 of multilinear regression parameters.

341 **Rate order and kinetic constant determination for the photodegradation of Multilinear regression parameters**

342 (A^{WW*0} , A^{WW*1} , A^{WW*2})

343 Kinetic constant and rate order of these parameters indicate how contribution of each PARAFAC component (Eq.2)
344 will evolve with irradiation time; hence EEM at any given point of irradiation time can be reconstructed. All irradiation
345 experiment (Exp.1, Exp.2, Exp.3 and Exp.4) showed continuous decrease of fluorescence signal with irradiation time
346 as shown in Fig.10. In comparison to other studies (Song et al. 2015; Zhu et al. 2017a), there was no increase of
347 fluorescence intensity found in this study. The decrease in values of (A^{WW*0} , A^{WW*1} , A^{WW*2}) in all experiments
348 could be fit by second order reaction kinetics (Table 5) in agreement with previous works (Yang et al. 2014). Moreover,
349 values of kinetic constant (k) are presented in Fig.11(a). Wu et al. (2016) found pseudo-first order reaction kinetics for
350 the removal of fluorescence region volumes using fluorescence regional integration “FRI” which is in contrast with
351 our study where fluorescence EEMs were modelled by PARAFAC and multilinear regression was conducted between
352 f_{SW} and f_{RW} and (C1, C2 and C3). In addition, those authors used simulated solar light during 12h and under 2.80
353 mW/cm² (visible) and 70.00 mW/cm². Second order reaction kinetics suggest that organic matter reacts with excited
354 organic matter itself. Values of kinetic constant for (A^{WW*0} , A^{WW*1} , A^{WW*2}) are shown in Fig.11(a). It can be seen
355 from Fig.11(a) that values of kinetic constant for intercept A^{WW*0} (Fig.10 a.1) is greater in C1 in Exp.1 compared to
356 the remaining experiment and also in comparison to A^{WW*2} and A^{WW*3} . In addition, same pattern can be seen in
357 Exp.3. Whereas for Exp.4 and Exp. 2, values of kinetic constant of A^{WW*0} , A^{WW*2} and A^{WW*3} are almost near zero
358 which are negligible. For kinetic constant k of A^{WW*1} , A^{WW*2} and A^{WW*3} (representing the impact of f_{SW}) (Fig.11
359 a.2) showed similar trend in Exp.1 and Exp.3 compared to Exp. 4 and Exp. 2 (their values also negligible). Moreover,
360 kinetic constant k of A^{WW*1} , A^{WW*2} and A^{WW*3} (representing the impact of f_{RW}) are shown in Fig.11 (a.3). Same trend
361 can be seen as mentioned above however with higher values of k compared to values of k for A^{WW*1} , A^{WW*2} and
362 A^{WW*3} . Negative values for k in the middle and right figures represent the negative impact of f_{SW} and f_{RW} on
363 fluorescence signal of C1, C2 and C3. The higher values of k for the coefficient of f_{RW} suggest that increasing the
364 percentage of river water in sample leads to faster photodegradation than increasing f_{SW} concentration in sample. The
365 lowest values of k for all C1, C2 and C3 are found for A^{WW*0} , A^{WW*2} and A^{WW*3} which are the intercept of multilinear
366 regression and implicitly retain information about the impact of f_{WW} . This suggests that increasing f_{WW} in sample retards
367 photodegradation of PARAFAC component. Photosensitivity variations are present between f_{WW} and f_{RW} or f_{SW} .

368 Accordingly, f_{WW} contribution is refractory and resilient under long irradiation. Zhu et al. (2017b) found similar results
369 between mixing of terrestrial and autochthonous organic matter. Wu et al. (2016) observed little variations between
370 humic-like and protein-like fluorophores in reclaimed water under strong conditions of irradiation. Kinetic constant
371 (k) is highest when SPOM of WW and SW were present (Exp.1 and Exp.3) which imply that SPOM from these WW
372 and SW makes the photodegradation faster for C1 and C2 and C3. Impact of SPOM from RW, SW and WW varies
373 according to fluorescent PARAFAC component. The nature of these SPOM should be investigated more in order to
374 understand their role in photodegradation. Advanced SPOM separation or extraction and fractionation techniques
375 should be used (e.g. XAD resins). Evolution with irradiation of initial values of (A^{WW*0} , A^{WW*1} , A^{WW*2}) before
376 irradiation for each corresponding PARAFAC component can be tracked using the values of their corresponding
377 kinetic constants hence reconstruction of fluorescence signal of C1, C2, and C3 can be conducted hence the whole
378 EEM of sample. Therefore, a dynamic model has been developed for the photodegradation of SPOM from different
379 water types. No clear behavior for control dark samples was found due to biological activity (Yang et al. 2014); except
380 the mean contributions relative deviation standard (RSD) and this is consistent with results shown above in Fig.10.
381 Relative Standard deviation (RSD) of parameters of multilinear regression are shown in Fig.11(b). RSD values in
382 Exp.4 are the smallest compared to all other irradiation experiments. This finding could be due to synergic effect of
383 the microbial activity coming simultaneously from all the water types (RW, SW and WW). RSD values for C3
384 coefficients of multilinear regression are higher for all irradiation experiments compared to those of C1 and C2. The
385 greater RSD value of C3 for all coefficients can be interpreted as having chaotic variations. Another observation is
386 that RSD values for C1 and C2 have an order of Exp. 1 > Exp. 2 > Exp. 3 > Exp. 4. SPOM from WW seems to be
387 responsible for variation with a greater degree compared to SPOM from SW and RW. Compared to irradiation
388 experiment (Exp.4), the synergistic effect of all SPOM makes RSD values to be the smallest possible. This observation
389 could be attributed to the fact that SPOM from each water type and microorganisms are competing which therefore
390 stabilize fluorescence signal in non-sterile dark control. These data indicate statistical differences between control
391 group and those exposed to sunlight during different time of year.

392 **Conclusions**

393 The rationale of this study emerges from the need to develop previous models for the prediction of fluorescence signal
394 of anthropogenic DOM based on mixing composition of sample and to study the impact of presence/absence of
395 suspended particulate matter of three water types (River water RW, Seawater SW, effluent wastewater WW) on the
396 resulting fluorescence signal of their mixtures and to simulate their natural mixing. Four Mixing and Irradiation
397 Experiments (Exp.1, Exp.2, Exp.3 and Exp.4) were conducted during different time of year and the impact of

398 irradiation and presence/absence of suspended particulate matter from three water types (river water RW, seawater
399 SW, effluent wastewater WW) were studied using three-dimensional fluorescence spectroscopy coupled with parallel
400 factor analysis EEM-PARAFAC. Evolution of fluorescence signal of PARAFAC components was investigated
401 kinetically through kinetic evolution of multilinear regression parameters with irradiation. Three components (C1,C2
402 and C3) might be extracted from the whole EEM dataset of all irradiation experiments. Protein-like component might
403 not be found which is due to its very low fluorescence intensity in the whole dataset. Second order kinetics were found
404 for all parameters (intercept , coefficient of f_{SW} and coefficient of f_{RW}) indicating bimodal reaction of organic matter
405 with itself and excited organic matter. It can be concluded that SPOM of one water type has profound impact on the
406 resulting kinetic constants of multilinear regression parameters. Kinetic constants of (A^{WW*0} “i.e. intercept” , A^{WW*1}
407 “coefficient of f_{SW} ” and A^{WW*2} “coefficient of f_{RW} ”) were the highest in irradiation experiment Exp. 1 and Exp. 3 and
408 the lowest in Exp. 4 and Exp.2. Thus, this study is a further step on the development of online or real time models of
409 evolution of fluorescence signal coming from anthropogenic sources. Further studies are warranted for the application
410 of this model on other urban river systems.

411 **Acknowledgements**

412 This work was funded by Hermes Program – from European commission through its Erasmus Mundus foundation; in
413 addition to the funding from Campus France through its research grant Al Maqdisi PHC Project n° 40229SD.
414 Moreover, we are thankful toward Christian Martino and Gael Durrieu for being available in each sampling campaign.

415 **Compliance with ethical standards**

416 **Conflict of interest**

417 The authors declare no conflict of interest

418 **Author Contributions**

419 **Ibrahim EL-Nahhal:** Funding acquisition, Conceptualization, Methodology, Writing- Reviewing and Editing **Ro-**
420 **land Redon:** Software -Reviewing **Michel Raynaud:** Software -Reviewing **Yasser EL-Nahhal:** Funding acquisition,
421 Reviewing and Editing **Stéphane Mounier:** Funding acquisition, Supervision, Project administration, Reviewing and
422 Editing. All authors read and approved the final manuscript.

423 **References**

- 424 Abaker M G, Domeizel M, Mouloubou O R, Rapetti N, Mounier S (2018) UV–Visible and Fluorescence Green Waste
425 Composts Monitoring: Material Dependency. *Compost Sci Util* 26(3):177–188.
426 <https://doi.org/10.1080/1065657X.2018.1434023>
427 Akkanen J, Vogt R D, Kukkonen J V K (2004) Essential characteristics of natural dissolved organic matter affecting

428 the sorption of hydrophobic organic contaminants. *Aquat Sci* 66:171–177. <https://doi.org/10.1007/s00027-004->
429 0705-x

430 Baker A, Spencer R G M (2004) Characterization of dissolved organic matter from source to sea using fluorescence
431 and absorbance spectroscopy. *Sci Total Environ* 33:217–232. <https://doi.org/10.1016/j.scitotenv.2004.04.013>

432 Baker A, Tipping E, Thacker S A, Gondar D (2008). Relating dissolved organic matter fluorescence and functional
433 properties. *Chemosphere* 73(11):1765–1772. <https://doi.org/10.1016/j.chemosphere.2008.09.018>

434 Boyd T J, Osburn C L (2004) Changes in CDOM fluorescence from allochthonous and autochthonous sources during
435 tidal mixing and bacterial degradation in two coastal estuaries. *Mar Chem* 89:189–210.
436 <https://doi.org/10.1016/j.marchem.2004.02.012>

437 Bro R 1998 Multi-way Analysis in the Food Industry. Ph.D. dissertation, University of Amsterdam. Retrieved from :
438 http://www.models.kvl.dk/sites/default/files/brothesis_0.pdf

439 Callahan J, Dai M, Chen R F, Li X, Lu Z, Huang W (2004) Distribution of dissolved organic matter in the Pearl river
440 estuary, China. *Mar Chem* 89:211–224. <https://doi.org/10.1016/j.marchem.2004.02.013>

441 Chin W C, Orellana M V, Verdugo P (1998). Spontaneous assembly of marine dissolved organic matter into polymer
442 gels. *Nature* 391:568–572. <https://doi.org/10.1038/35345>

443 Coble P G (1996) Characterization of marine and terrestrial DOM in seawater using excitation-emission matrix spec-
444 troscopy. *Mar Chem* 51(4):325–346. [https://doi.org/10.1016/0304-4203\(95\)00062-3](https://doi.org/10.1016/0304-4203(95)00062-3)

445 Cohen E, Levy G J, Borisover M (2014) Fluorescent components of organic matter in wastewater: efficacy and selec-
446 tivity of the water treatment. *Water Res* 55:323–334. <https://doi.org/10.1016/j.watres.2014.02.040>

447 Dalzell B J, Minor E C, Mopper K M (2009) Photodegradation of estuarine dissolved organic matter: an assessment
448 of DOM transformation. *Org Geochem* 40:253–257. <https://doi.org/10.1016/j.orggeochem.2008.10.003>

449 De Souza Sierra M M, Donard O F X (1991) Simulation of fluorescence variability in estuaries. *Oceanologica Acta*
450 11:275–284

451 EL-Nahhal I, Redon R, Raynaud M, EL-Nahhal Y, Mounier S (2020) Characterization of the fate and changes of post-
452 irradiance fluorescence signal of filtered anthropogenic effluent dissolved organic matter from wastewater treat-
453 ment plant in the coastal zone of Gapeau river. *Environ Sci Pollut Res* 27:23141–23158
454 <https://doi.org/10.1007/s11356-020-08842-w>

455 El-Nahhal Y, Nir S, Margulies L, Rubin B (1999) Reduction of photodegradation and volatilization of herbicides in
456 organo-clay formulations. *Appl Clay Sci* 14:105-119. [https://doi.org/10.1016/S0169-1317\(98\)00053-2](https://doi.org/10.1016/S0169-1317(98)00053-2)

457 Estapa M L, Mayer L M (2010) Photooxidation of particulate organic matter, carbon/oxygen stoichiometry, and

458 related photoreactions. *Mar Chem* 122(1e4):138-147. <https://doi.org/10.1016/j.marchem.2010.06.003>

459 Gagné J P, Tremblay L (2009) Organic matter distribution and reactivity in the waters of a large estuarine system. *Mar*
460 *Chem* 116(1-4):1-12. <https://doi.org/10.1016/j.marchem.2009.09.006>

461 He W, Chen M, Schlautman M A, Hur J (2016) Dynamic exchanges between DOM and POM pools in coastal and
462 inland aquatic ecosystems: A review. *Sci Total Environ* 551-552:415–428. <https://doi.org/10.1016/j.scitotenv.2016.02.031>

463

464 Her N, Amy G, McKnight D, Sohn J, Yoon Y (2003) Characterization of DOM as a function of MW by fluorescence
465 EEM and HPLC-SEC using UVA, DOC, and fluorescence detection. *Water Res* 37(17):4295–4303.
466 [https://doi.org/10.1016/S0043-1354\(03\)00317-8](https://doi.org/10.1016/S0043-1354(03)00317-8)

467 Hirose K (2007) Metal–organic matter interaction: ecological roles of ligands in oceanic DOM. *Appl Geochem*
468 22:1636–1645. <https://doi.org/10.1016/j.apgeochem.2007.03.042>

469 Ishii S K, Boyer T H (2012) Behavior of reoccurring PARAFAC components in fluorescent dissolved organic matter
470 in natural and engineered systems: a critical review. *Environ Sci Technol* 46(4):2006–2017.
471 <https://doi.org/10.1021/es2043504>

472 Kowalczyk P, Cooper W J, Whitehead R F, Durako M J, Sheldon W (2003) Characterization of CDOM in an organic-
473 rich river and surrounding coastal ocean in South Atlantic Bight. *Aquat Sci* 65:384–401.
474 <https://doi.org/10.1007/s00027-003-0678-1>

475 Laane R W P M, Kramer K J M (1990) Natural fluorescence in the North Sea and its major estuaries. *Netherlands J*
476 *Sea Res* 26:1–9. [https://doi.org/10.1016/0077-7579\(90\)90052-I](https://doi.org/10.1016/0077-7579(90)90052-I)

477 Lapiere J F, del Giorgio P A (2014) Partial coupling and differential regulation of biologically and photochemically
478 labile dissolved organic carbon across boreal aquatic networks. *Biogeosciences* 11(20):5969–5985.
479 <https://doi.org/10.5194/bg-11-5969-2014>

480 Lawaetz A J, Stedmon C A (2009) Fluorescence intensity calibration using the Raman scatter peak of water. *Appl*
481 *Spectrosc* 63(8):936–940. <https://doi.org/10.1366/000370209788964548>

482 Leppard GG, West MM, Flannigan DT, Carson J, Lott J (2011) A classification scheme for marine organic colloids
483 in the Adriatic Sea: colloid speciation by transmission electron microscopy. *Can J Fish Aquat Sci* 54(10):2334–
484 2349

485 Liu Q Y, Shank G C (2015) Solar radiation-enhanced dissolution (photodissolution) of particulate organic matter in
486 Texas estuaries. *Estuaries Coasts* 38 (6):2172-2184. <https://doi.org/10.1007/s12237-014-9932-0>

487 Lopez L M, Croce E A, Sicre E J (1998) The photochemical reaction between chlorine and chlorine perchlorate at
488 366 nm *J Photochem Photobiol A Chem* 112:97-102. [https://doi.org/10.1016/S1010-6030\(97\)00276-1](https://doi.org/10.1016/S1010-6030(97)00276-1)

489 Margulies L, Rosen H, Stern T, Rytwo G, Rubin B, Ruso L, Nir S, Cohen E (1993) Photostabilization of pesticides
490 by clays and chromophores. *Arch Insect Biochem Physiol* 22:467–486. <https://doi.org/10.1002/arch.940220313>

491 Mayer L M, Schick L L, Skorko K, Boss E (2006) Photodissolution of particulate organic matter from sediments.
492 *Limnol Oceanogr* 51 (2):1064-1071. <https://doi.org/10.4319/lo.2006.51.2.1064>

493 McCallister S L, Bauer J E, Canuel E A (2006a) Bioreactivity of estuarine dissolved organic matter: A combined
494 geochemical and microbiological approach. *Limnol Oceanogr* 51(1):94–100.
495 <https://doi.org/10.4319/lo.2006.51.1.0094>

496 McCallister S L, Bauer J E, Ducklow H W, Canuel E A (2006b) Sources of estuarine dissolved and particulate organic
497 matter: A multi-tracer approach. *Org Geochem* 37(4):454–468. [https://doi.org/10.1016/J.ORGGEO-](https://doi.org/10.1016/J.ORGGEO-CHEM.2005.12.005)
498 [CHEM.2005.12.005](https://doi.org/10.1016/J.ORGGEO-CHEM.2005.12.005)

499 Micó P, García-Ballesteros S, Mora M, Vicente R, Amat A M, Arques A (2019) EEMlab: A graphical user-friendly
500 interface for fluorimetry experiments based on the drEEM toolbox. *Chemometr Intell Lab Syst* 188:6–13.
501 <https://doi.org/10.1016/J.CHEMOLAB.2019.03.001>

502 Mopper K, Kieber D J, Stubbins A (2014) Marine Photochemistry of Organic Matter: Processes and Impacts. Pro-
503 cesses and Impacts. In *Biogeochemistry of Marine Dissolved Organic Matter: Second Edition* (pp. 389–450).
504 <https://doi.org/10.1016/B978-0-12-405940-5.00008-X>

505 Morris J C (1978) The chemistry of aqueous chlorine in relation to water chlorination. In: Jolleys, R.L. (Ed.), *Water*
506 *Chlorination: Environmental Impact and Health Effects*, vol. 1. Ann Arbor Science Publishers, Michigan, pp.
507 21–35.

508 Muellner M G, Wagner E D, Mccalla K, Richardson S D, Woo Y T, Plewa M J (2007) Haloacetonitriles vs. regulated
509 haloacetic acids: are nitrogen-containing DBFs more toxic? *Environ Sci Technol* 41(2):645-651.
510 <https://doi.org/10.1021/es0617441>

511 Murphy K R, Hambly A, Singh S, Henderson R K, Baker A, Stuetz R, Khan S J (2011) Organic Matter Fluorescence
512 in Municipal Water Recycling Schemes: Toward a Unified PARAFAC Model. *Environ Sci Technol* 45(7):2909–
513 2916. <https://doi.org/10.1021/es103015e>

514 Murphy K R, Stedmon C A, Graeber D, Bro R (2013) Fluorescence spectroscopy and multi-way techniques. PARA-
515 FAC. *Anal Methods* 5(23):6557. <https://doi.org/10.1039/c3ay41160e>

516 Murphy K R, Stedmon C A, Waite T D, Ruiz G M (2008) Distinguishing between terrestrial and autochthonous

517 organic matter sources in marine environments using fluorescence spectroscopy. *Mar Chem* 108(1–2):40–58.
518 <https://doi.org/10.1016/j.marchem.2007.10.003>

519 Nir S, Undabeytia T, Yaron D, El-Nahhal Y, Polubesova T, Serban S, Rytwo G, Lagaly G, Rubin B (2000)
520 Optimization of adsorption of hydrophobic herbicides on montmorillonite preadsorbed by monovalent organic
521 cations: Interaction between phenyl rings. *Environ Sci Technol* 34:1269–1274.
522 <https://doi.org/10.1021/es9903781>

523 Ohno T (2002) Fluorescence inner-filtering correction for determining the humification index of dissolved organic
524 matter. *Environ Sci Technol* 36(4):742–746. <https://doi.org/10.1021/es0155276>

525 Osburn C L, Handsel L T, Mikan M P, Paerl H W, Montgomery M T (2012) Fluorescence tracking of dissolved and
526 particulate organic matter quality in a river-dominated estuary. *Environ Sci Technol* 46(16):8628–8636.
527 <https://doi.org/10.1021/es3007723>

528 Parlanti E, Wörz K, Geoffroy L, Lamotte M (2000) Dissolved organic matter fluorescence spectroscopy as a tool to
529 estimate biological activity in a coastal zone submitted to anthropogenic inputs. *Org Geochem* 31(12):1765–
530 1781. [https://doi.org/10.1016/S0146-6380\(00\)00124-8](https://doi.org/10.1016/S0146-6380(00)00124-8)

531 Patel-Sorrentino N, Mounier S, Benaim J Y (2002) Excitation-emission fluorescence matrix to study pH influence on
532 organic matter fluorescence in the Amazon basin rivers. *Water Res* 36(10):2571–2581.
533 [https://doi.org/10.1016/s0043-1354\(01\)00469-9](https://doi.org/10.1016/s0043-1354(01)00469-9)

534 Péron A, Courtot-Coupez J (1980) Etude physicochimique de la chloration de l'eau de mer artificielle. *Water Res*
535 14(4):329–332. [https://doi.org/10.1016/0043-1354\(80\)90079-2](https://doi.org/10.1016/0043-1354(80)90079-2)

536 Pisani O, Yamashita Y, Jaffe R (2011) Photo-dissolution of flocculent, detrital material in aquatic environments:
537 contributions to the dissolved organic matter pool. *Water Res* 45 (13):3836–3844.
538 <https://doi.org/10.1016/j.watres.2011.04.035>

539 Riggsbee J A, Orr C H, Leech D M, Doyle M W, Wetzel R G (2008) Suspended sediments in river ecosystems:
540 photochemical sources of dissolved organic carbon, dissolved organic nitrogen, and adsorptive removal of
541 dissolved iron. *J Geophys Research-Biogeosciences* 113(G3):019. <https://doi.org/10.1029/2007JG000654>

542 Seong-Nam N, Gary A (2008) Differentiation of Wastewater Effluent Organic Matter (EfOM) From Natural Organic
543 Matter (NOM) Using Multiple Analytical Techniques. *Water Sci Technol* 57(7).
544 <https://doi.org/10.2166/WST.2008.165>

545 Sgroi M, Gagliano E, Vagliasindi F, Roccaro P (2020) Inner filter effect, suspended solids and nitrite/nitrate interfer-
546 ences in fluorescence measurements of wastewater organic matter. *Sci Total Environ* 711:134663.

547 <https://doi.org/10.1016/j.scitotenv.2019.134663>

548 Søndergaard M, Thomas D N (2004) Dissolved Organic Matter (DOM) in Aquatic Ecosystems: A Study of European
549 Catchments and Coastal Waters. EU Project DOMAINE 87-89143-25-6.

550 Song W, Zhao C, Mu S, Pan X, Zhang D, Al-Misned F A, Mortuza M G (2015) Effects of irradiation and pH on
551 fluorescence properties and flocculation of extracellular polymeric substances from the cyanobacterium *Chroo-*
552 *coccus minutus*. *Colloids Surf B Biointerfaces* 128:115–118. <https://doi.org/10.1016/J.COLSURFB.2015.02.017>

553 Southwell M W, Kieber R J, Mead R N, Avery G B, Skrabal S A (2010) Effects of sunlight on the production of
554 dissolved organic and inorganic nutrients from resuspended sediments. *Biogeochemistry* 98(1-3):115-126.
555 <https://doi.org/10.1007/s10533-009-9380-2>

556 Stedmon C A, Bro R (2008) Characterizing dissolved organic matter fluorescence with parallel factor analysis: A
557 tutorial. *Limnol Oceanogr Methods / ASLO* 6(11):572–579. <https://doi.org/10.4319/lom.2008.6.572>

558 Stedmon C A, Markager S (2005) Resolving the variability in dissolved organic matter fluorescence in a temperate
559 estuary and its catchment using PARAFAC analysis. *Limnol Oceanogr* 50(2):686–697.
560 <https://doi.org/10.4319/lo.2005.50.2.0686>

561 Stedmon C A, Markager S, Bro R (2003) Tracing dissolved organic matter in aquatic environments using a new
562 approach to fluorescence spectroscopy. *Mar Chem* 82(3-4):239–254. [http://dx.doi.org/10.1016/s0304-](http://dx.doi.org/10.1016/s0304-4203(03)00072-0)
563 [4203\(03\)00072-0](http://dx.doi.org/10.1016/s0304-4203(03)00072-0)

564 Tucker S A, Amszi V L, Acree W E (1992) Primary and secondary inner filtering: effect of K₂Cr₂O₇ on fluorescence
565 emission intensities of quinine sulfate. *J Chem Educ* 69:A8–A12. <https://doi.org/10.1021/ed069pA8>

566 Wu Q, Li C, Wang W, He T, Hu H, Du Y, Wang T (2016) Removal of fluorescence and ultraviolet absorbance of
567 dissolved organic matter in reclaimed water by solar light. *J Environ Sci* 43:118–127.
568 <https://doi.org/10.1016/J.JES.2015.08.021>

569 Wünsch U J, Murphy K R, Stedmon C A (2017) The One-Sample PARAFAC Approach Reveals Molecular Size
570 Distributions of Fluorescent Components in Dissolved Organic Matter. *Environ Sci Technol* 51(20):11900–
571 11908. <https://doi.org/10.1021/acs.est.7b03260>

572 Yang X, Meng F, Huang G, Sun L, Lin Z (2014) Sunlight-induced changes in chromophores and fluorophores of
573 wastewater-derived organic matter in receiving waters – The role of salinity. *Water Res* 62:281–292.
574 <https://doi.org/10.1016/J.WATRES.2014.05.050>

575 Zepp R G, Sheldon W M, Moran M A (2004) Dissolved organic fluorophores in southeastern US coastal waters:
576 correction method for eliminating Rayleigh and Raman scattering peaks in excitation–emission matrices. *Mar*

577 Chem 89(1–4):15–36. <https://doi.org/10.1016/J.MARCHEM.2004.02.006>

578 Zhu W Z, Yang G P, Zhang H H (2017a) Photochemical behavior of dissolved and colloidal organic matter in estuarine
579 and oceanic waters. *Sci Total Environ* 607–608:214–224. <https://doi.org/10.1016/J.SCITOTENV.2017.06.163>

580 Zhu W Z, Zhang J, Yang G P (2017b) Mixing behavior and photobleaching of chromophoric dissolved organic matter
581 in the Changjiang River estuary and the adjacent East China Sea. *Estuar Coast Shelf Sci*
582 <https://doi.org/10.1016/J.ECSS.2017.07.019>

583

584

585

586

587

588

589

590

591

592

593 **Figures Captions**

594 **Fig. 1** Ternary diagram of the mixing percentages of three endmember mixing components (freshwater (RW),
595 wastewater treatment plant (WW), seawater (SW)). Each red point represents a solution that contains the men-
596 tioned and calculated percentages of each water source (endmember)

597 **Fig. 2** The used apparatus for all the irradiation experiments which was on the rooftop of MIO laboratory/ University
598 of Toulon-France. GPS location: (43° 08' 11.2" N 6° 01' 16.7" E)

599 **Fig. 3** Light intensity measured in millivolts mV for the four irradiation experiments

600 **Fig. 4** Linearity of UV-Vis absorbance spectra with dilution of the sampled 1L RW, 1L WW, 1L SW from top to
601 down respectively showing no Inner Filter Effect

602 **Fig. 5** EEMs of Samples 1,2,3 in Irradiation experiment Exp.1

603 **Fig. 6** EEMs of Samples 1,2,3 in irradiation experiment Exp.2

604 **Fig. 7** EEMs of Samples 1,2,3 in Irradiation experiment Exp.3

605 **Fig. 8** EEMs of Samples 1,2,3 in Irradiation experiment Exp.4

606 **Fig. 9** Fluorescence landscape of PARAFAC components identified from the decomposition of all EEM datasets on

607 the left. Spectral loadings of excitation and emission wavelengths of the identified PARAFAC in the present
608 study on the right. Excitation loading for CP/PARAC component are shown in solid lines whereas emission
609 loadings are shown in dotted lines

610 **Fig. 10** Changes in the maximum fluorescence intensity of all four PARAFAC components (C1, C2, C3 and C4)
611 during Irradiation experiment Exp.4 . All Exp.1, Exp.2, Exp.3 showed the same pattern

612 **Fig. 11 (a)** Kinetic constant for coefficients of multilinear regression for C1,C2 and C3 PARAFAC components. **(b)**
613 The relative standard deviation (RSD) values for all the multilinear regression coefficients (intercept, coefficient
614 of f_{sw} , coefficient of f_{rw}) for the control dark samples in all the irradiation experiments

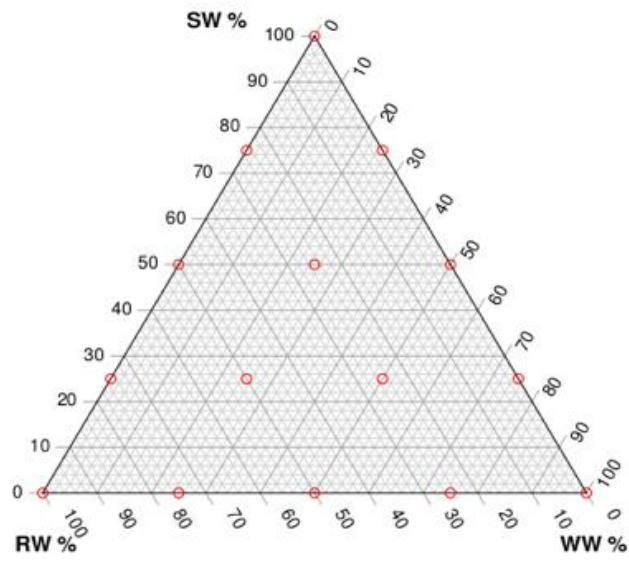
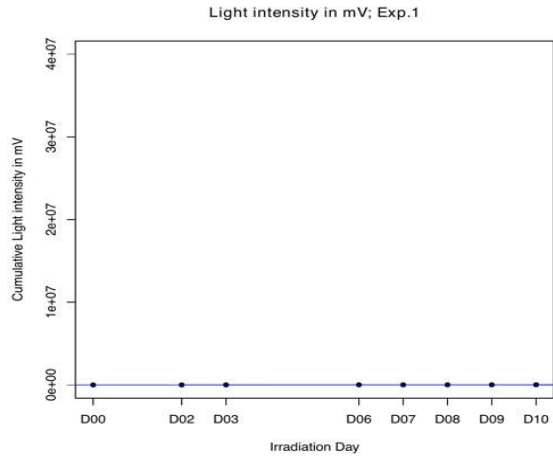


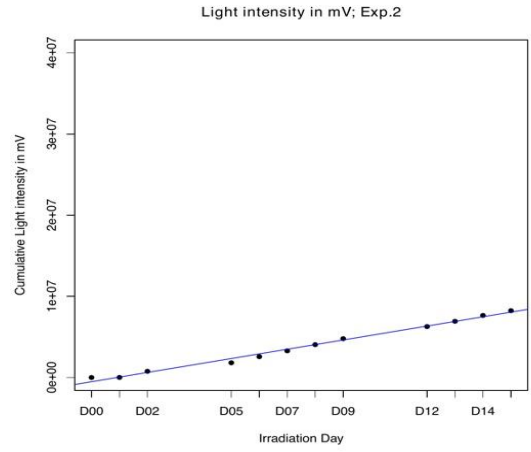
Fig. 1



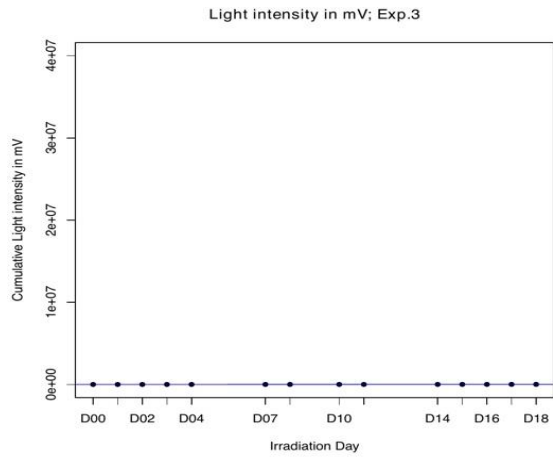
Fig. 2



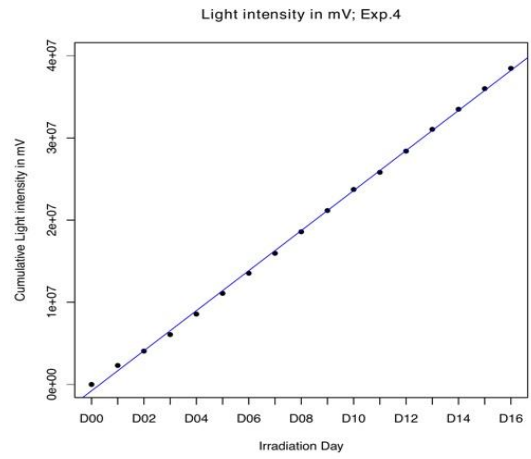
Exp.1 (Date: 10/11/2015 to 26/11/2015)



Exp.2 (Date: 02/12/2015 to 17/12/2015)



Exp.3 (Date: 15/02/2016 to 01/03/2016)



Exp.4 (Date: 11/05/2016 to 27/05/2016)

Fig. 3

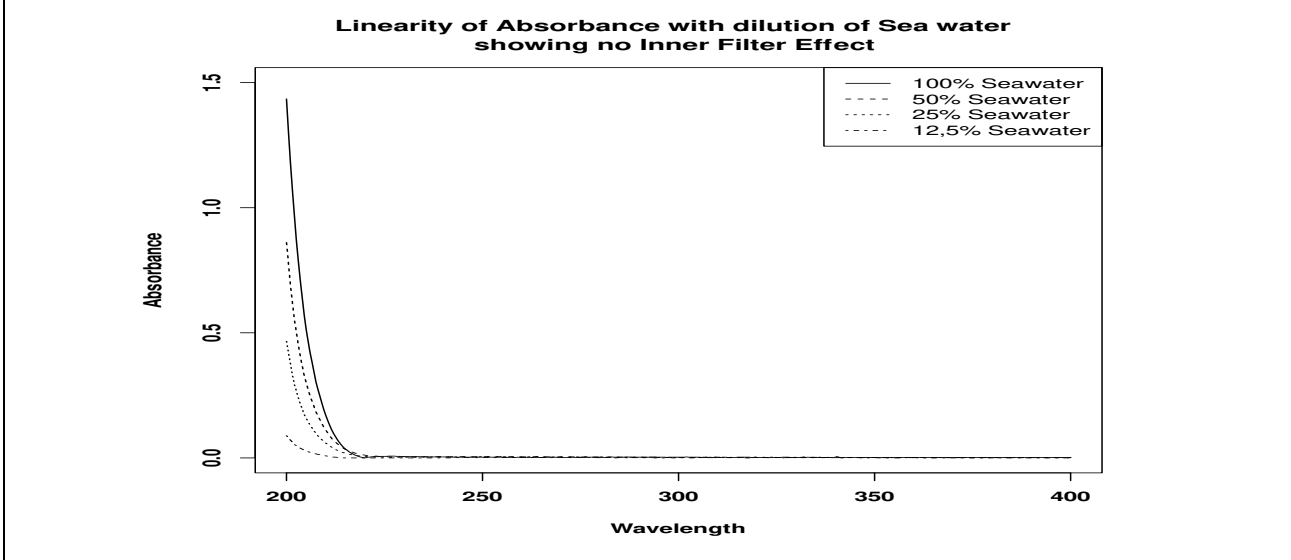
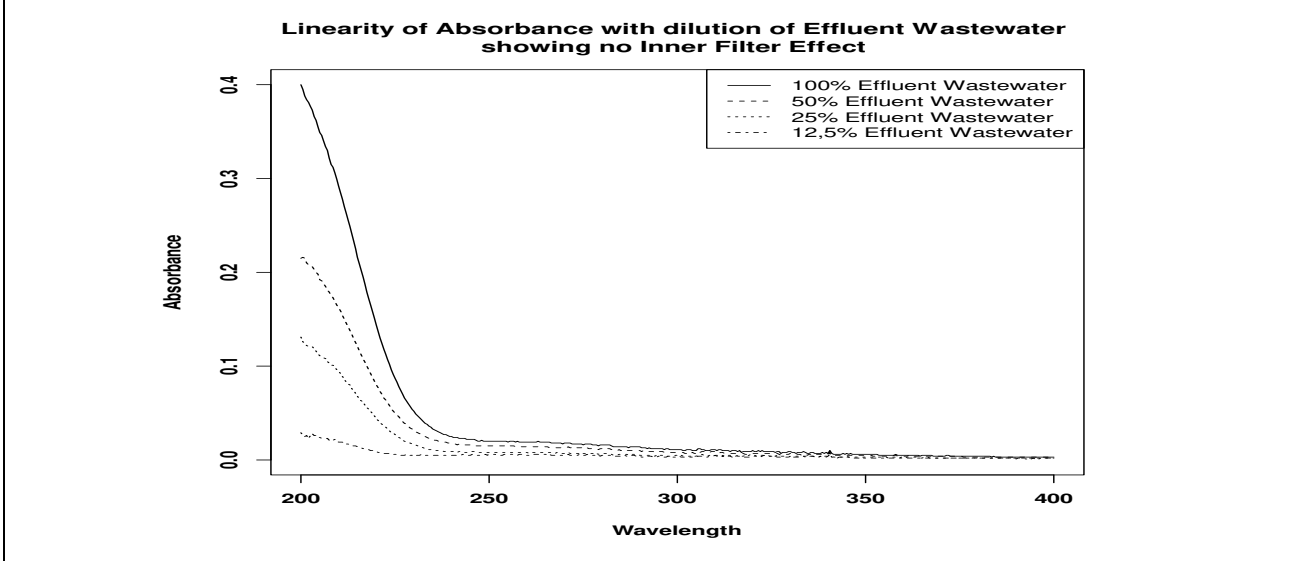
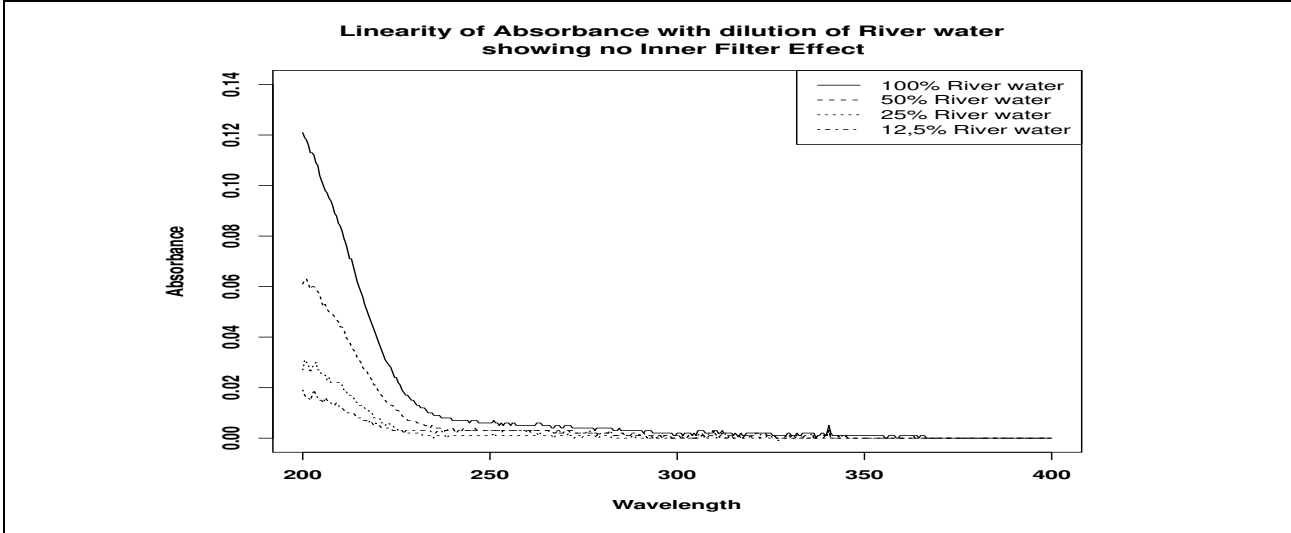
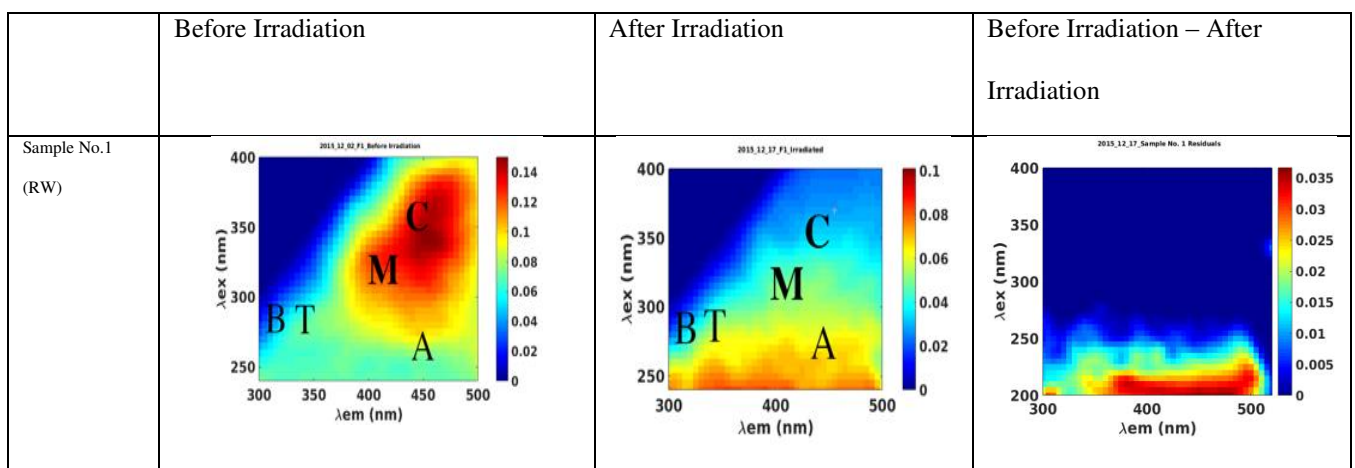
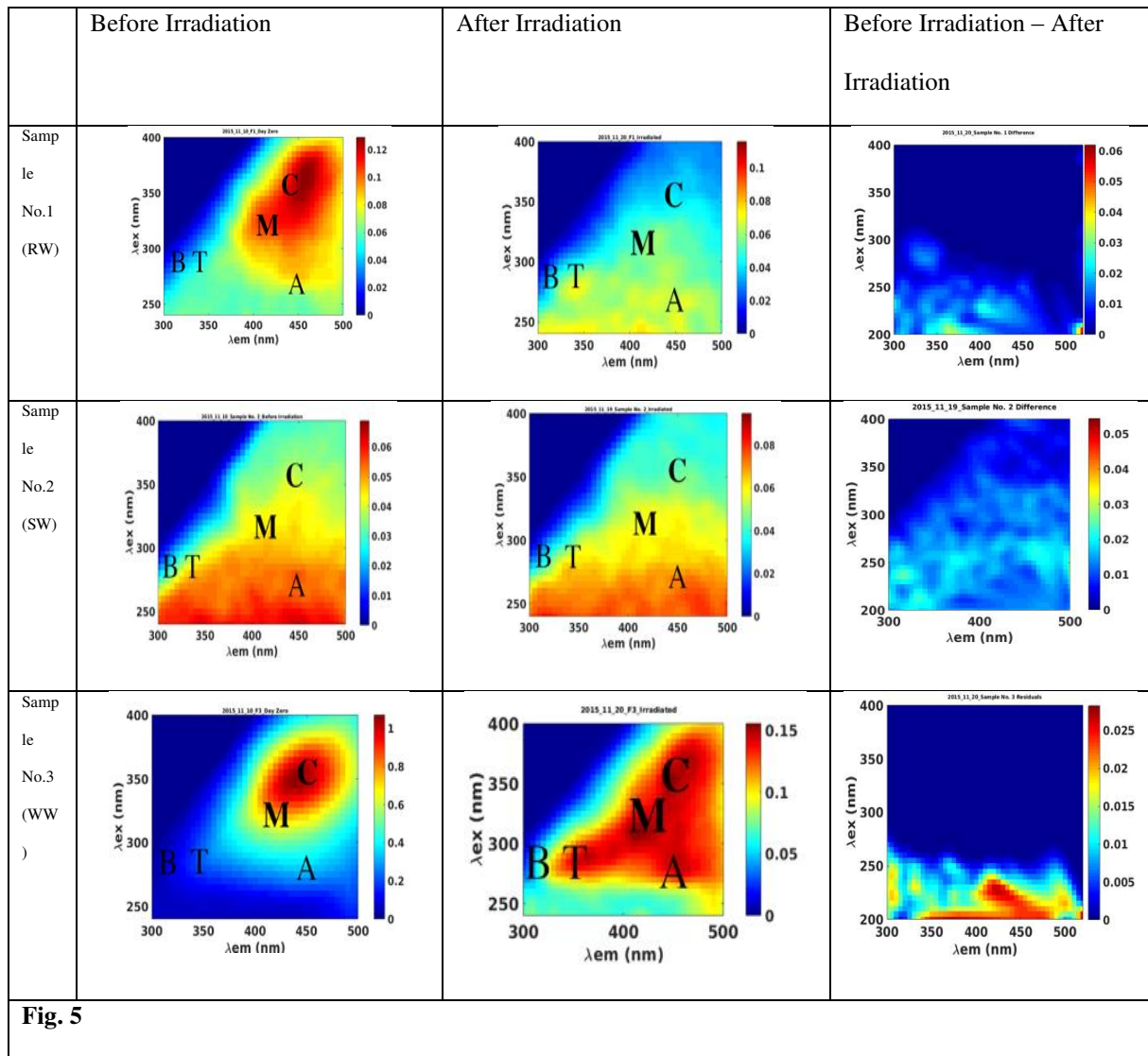


Fig. 4



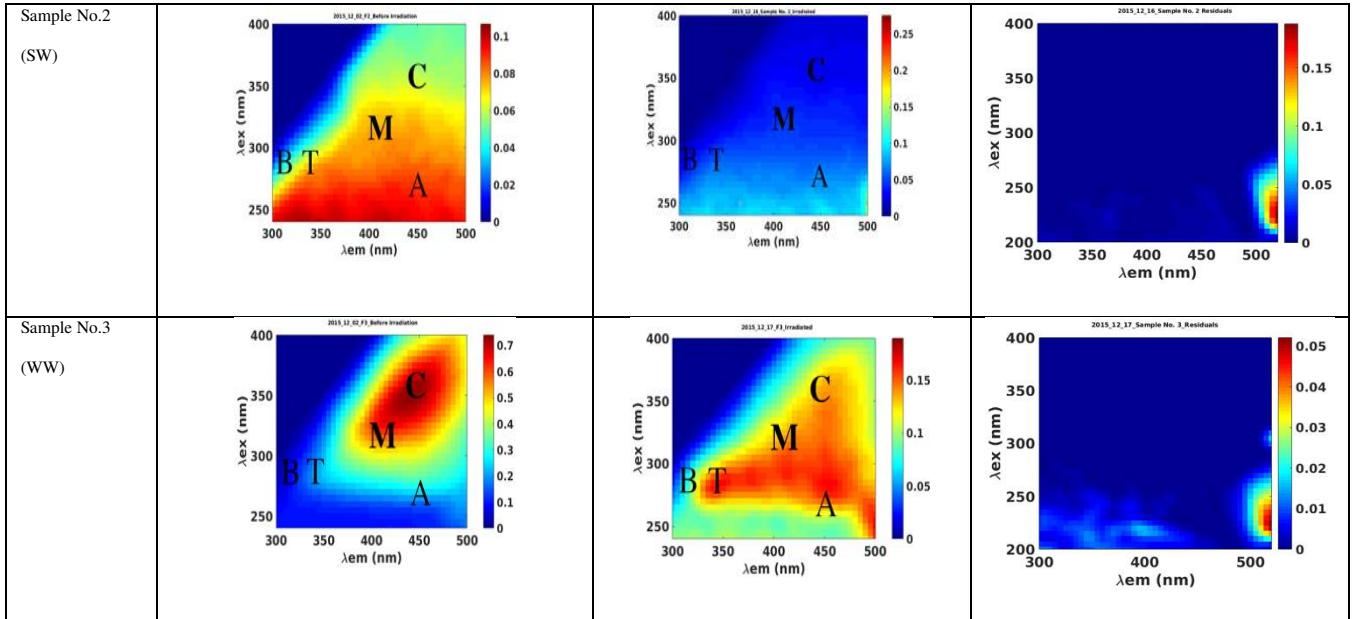


Fig. 6

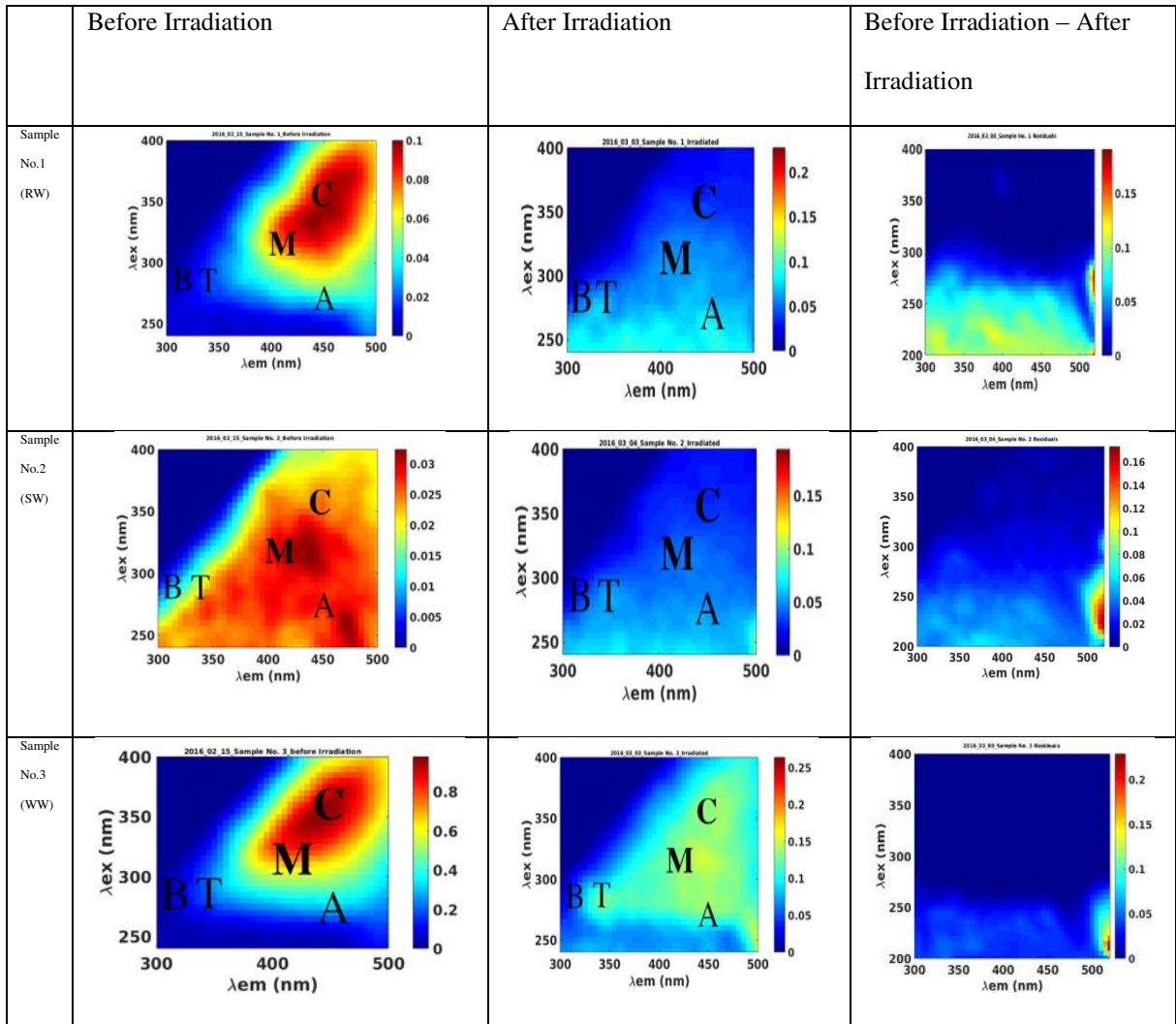


Fig. 7

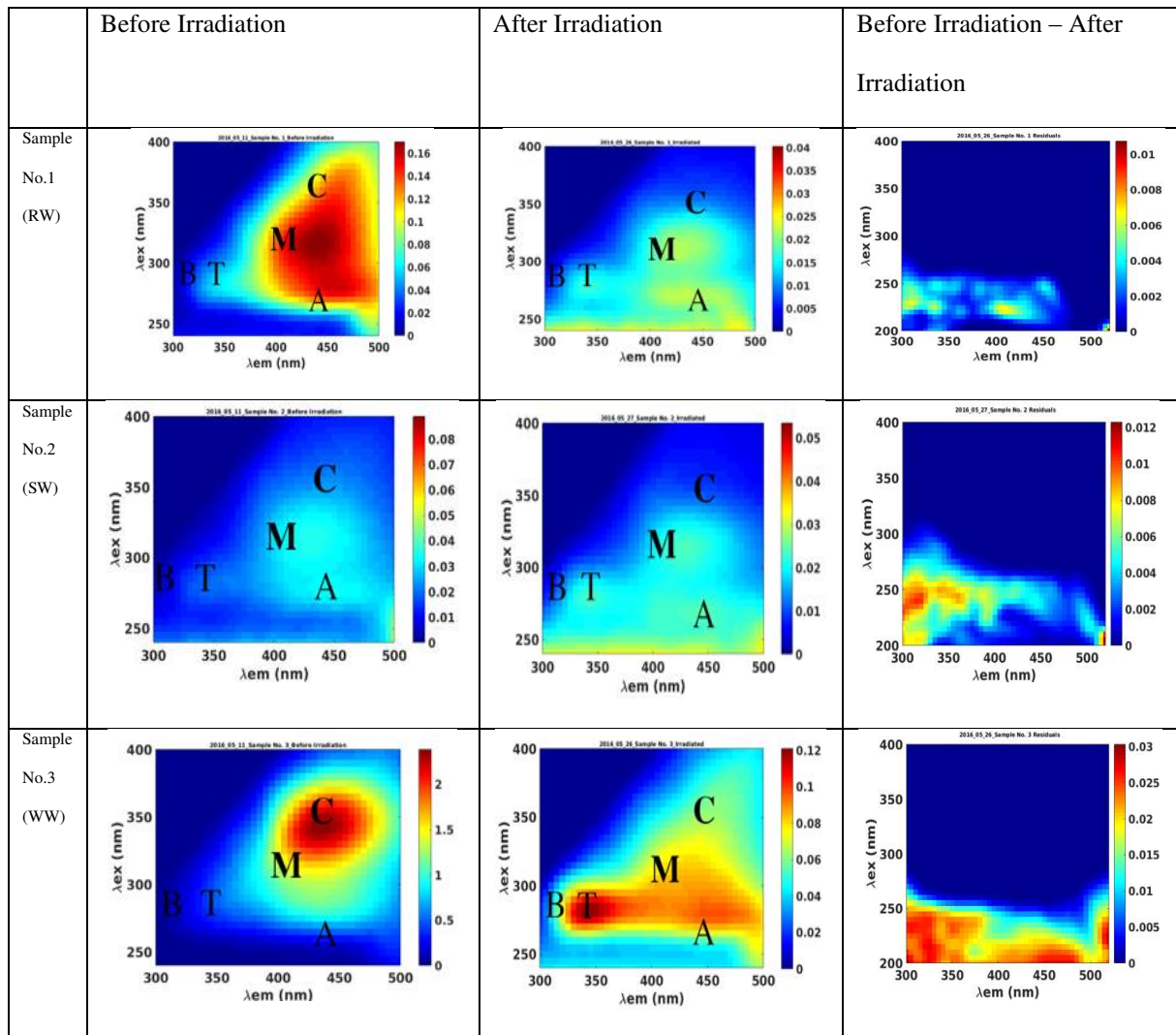
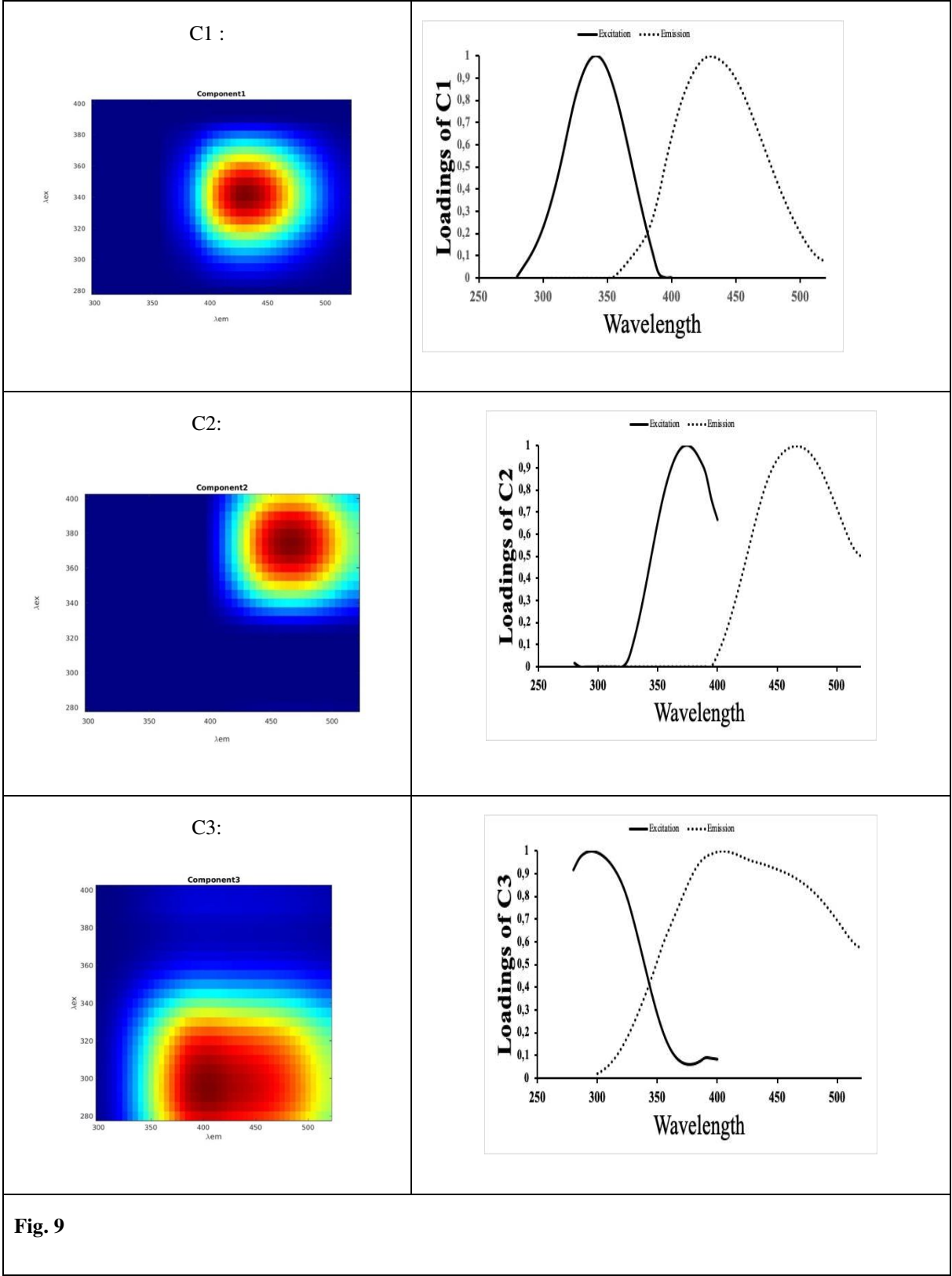
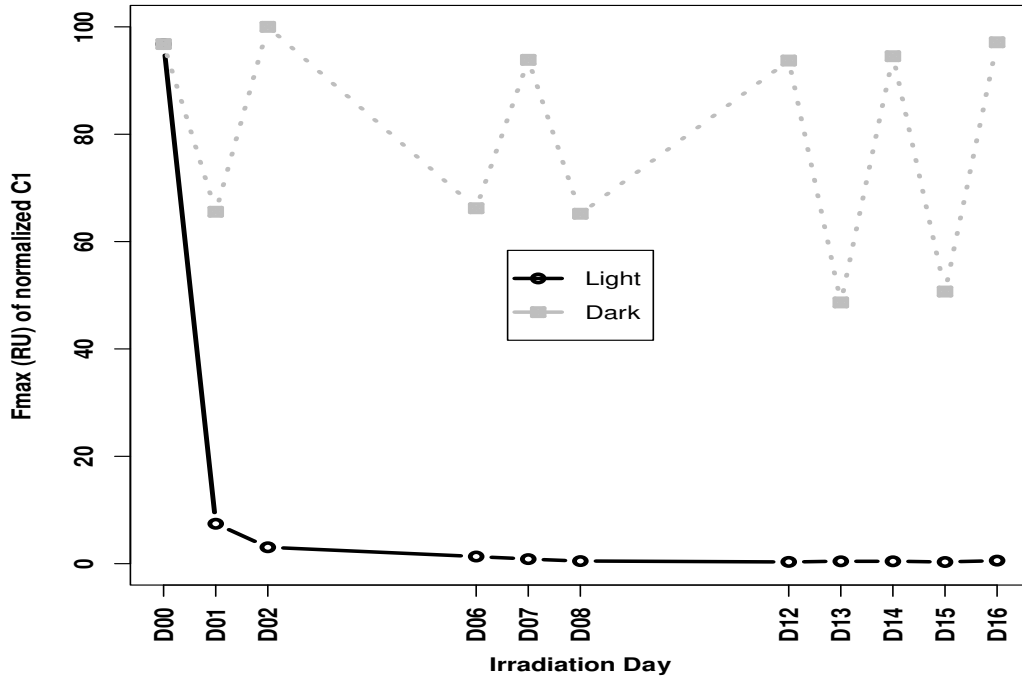


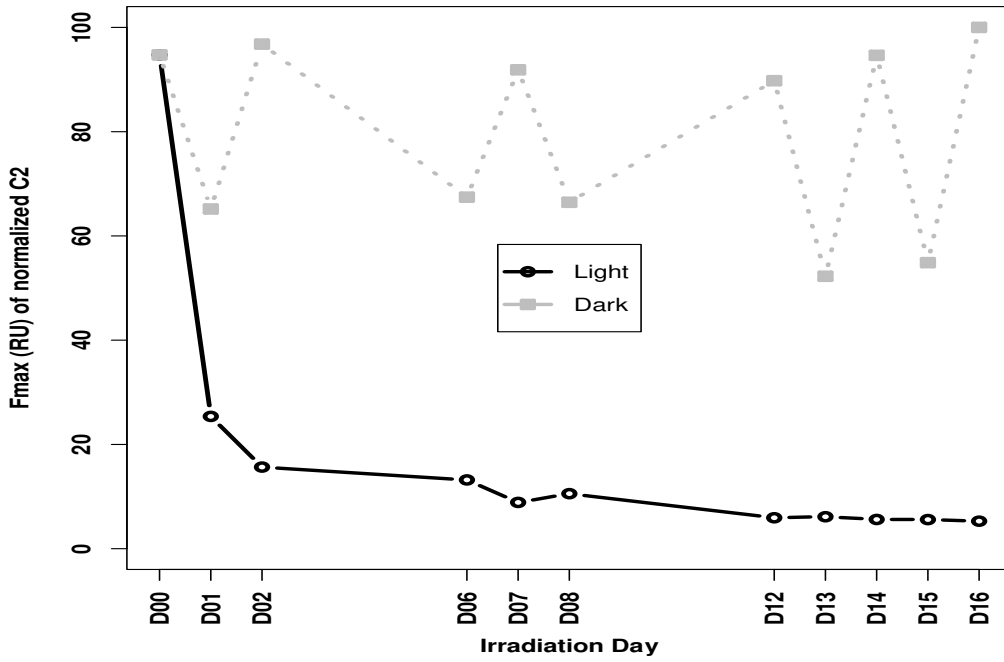
Fig. 8

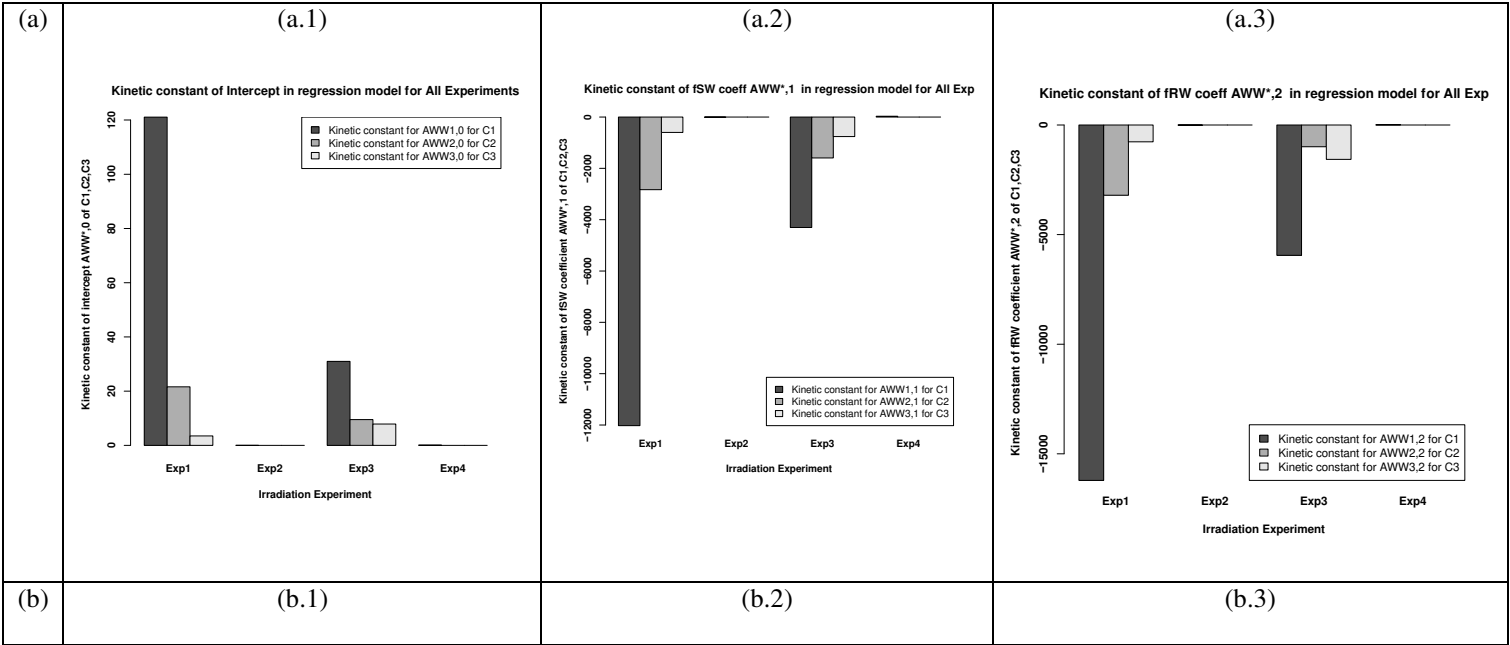
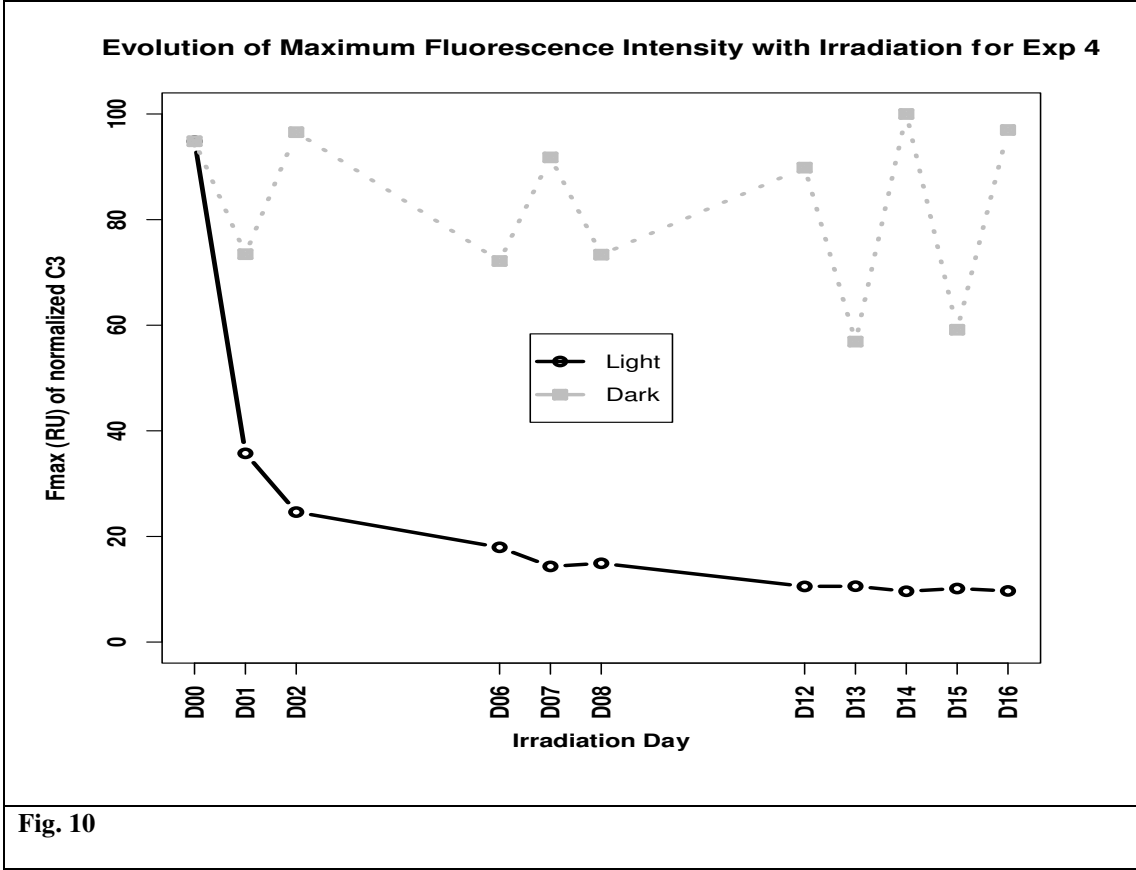


Evolution of Maximum Fluorescence Intensity with Irradiation for Exp 4



Evolution of Maximum Fluorescence Intensity with Irradiation for Exp 4





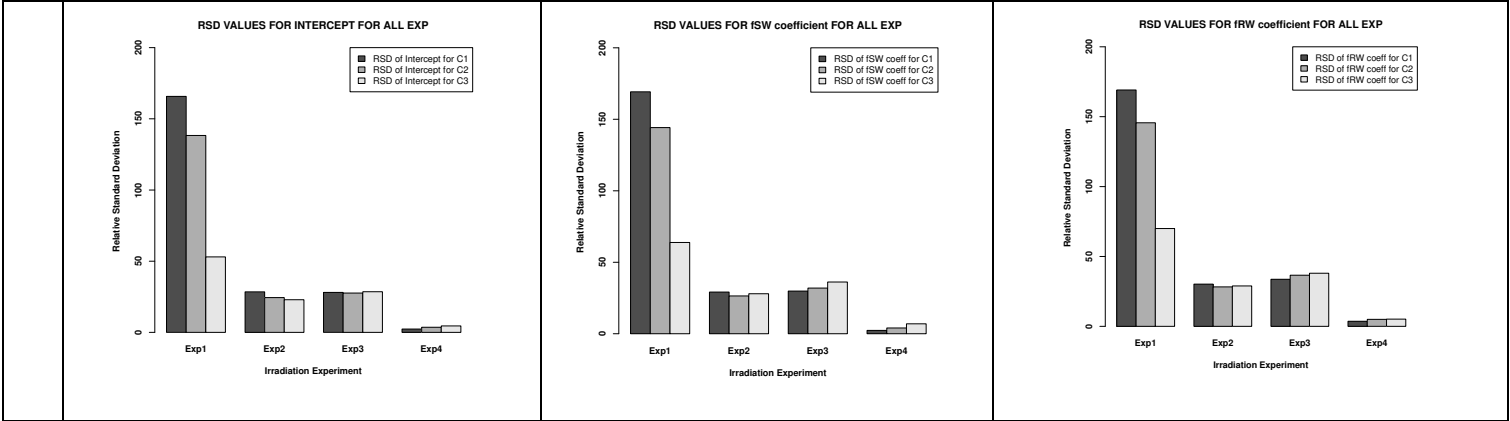


Fig. 11

Table 1

Exact volume in each quartz vial (indicated in its corresponding number) is the vertical sum in mL

Water type	Sample Number														
	1	2	3	4	5	6	7	8	9	10	11	12	13	14	15
RW	50	0	0	37.5	25	12.5	37.5	25	12.5	0	0	0	25	12.5	12.5
SW	0	50	0	12.5	25	37.5	0	0	0	12.5	25	37.5	12.5	12.5	25
WW	0	0	50	0	0	0	12.5	25	37.5	37.5	25	12.5	12.5	25	12.5

Table 2

Irradiation Experiments dates and types.

Experiment	Filtration state of RW, SW and WW	Irradiation Start Date	Irradiation End Date	Duration
Exp. 1	RW(F), SW(F), WW (NF)	10/11/2015	26/11/2015	16 days
Exp. 2	RW(NF), SW(F), WW(F)	02/12/2015	17/12/2015	16 days
Exp. 3	RW(F), SW(NF), WW(F)	15/02/2016	01/03/2016	16 days
Exp. 4	RW(NF), SW(NF), WW(NF)	11/05/2016	27/05/2016	16 days

F indicates filtered state and NF means Not Filtered state

Table 3

Correspondence of PARAFAC components in this study with components reported elsewhere in literature.

The present study			Correspondence with literature	Correspondence with openflour.org database
Component	Ex/Em (nm)	Characterization		
C1	340/430	Wastewater/nutrient enrichment tracer; terrestrial humic-like	G3(1) , Peak C (2), C4(3);	RecycleG7 C3; RecycleStM C1; RecycleWTP C3; RecycleWRAMS C4; RecycleRH C1; RecyclePC C3; Peleato_OzoneAOP_biofilter C1; MIEX-DOC-GOLD C2; Vines_WWEff C1; Fuirosos_Drought C2
C2	375/465	More humificated or ligneous compounds	Peak A (2); C ₄₅₀ (4); C2(7)	osPARAFAC_RioNegro C4; Masanbay_Korea C2; Partners C2; MIEX-DOC-GOLD C4; Drink C2; osPARAFAC_Lillsjoen C4
C3	295/405	Anthropogenic humic materials, agricultural; Microbial component	Peak M(2); C2(5);C5(6); C2(8)	FloridaKeys C1; Shutova_F C1; WAIS_Holocene_3 C3; NeusePOMDOM C2; Kauai C1; Vines_BWR C1; Fuirosos_Drought C1; Vines_WWEff C2; Shakil_Peel2015t2017_5comp C1; RaskaDOM C1; Arctic Seawater C2; Borisover_wastewater treatment plants C2; BengalBasin_GW_Nadia_Acidification C1

1. Murphy et al. (2011); 2. Coble (1996) ; 3. Lapierre and del Giorgio (2014); 4.Wünsch et al. (2017); 5.Murphy et al. (2008); 6.Stedmon and Markager (2005);7. Abaker et al. (2018); 8. Cohen et al., 2014

